UNIVERSIDAD DE CONCEPCIÓN

Centro de Investigación en
Ingeniería Matemática (CI^{2}MA)

Mathematical and numerical analysis of a transient eddy current axisymmetric problem involving velocity terms

Alfredo Bermúdez, Carlos Reales,
Rodolfo Rodríguez, Pilar Salgado

PREPRINT 2010-04

SERIE DE PRE-PUBLICACIONES

MATHEMATICAL AND NUMERICAL ANALYSIS OF A TRANSIENT EDDY CURRENT AXISYMMETRIC PROBLEM INVOLVING VELOCITY TERMS.

ALFREDO BERMÚDEZ, CARLOS REALES, RODOLFO RODRÍGUEZ,
AND PILAR SALGADO

ABSTRACT. The aim of this paper is to analyze a transient axisymmetric electromagnetic model involving velocity terms in the Ohm's law. To this end we introduce a time-dependent weak formulation leading to a degenerate parabolic problem and establish its well-posedness. We propose a finite element method for space discretization and prove well-posedness and error estimates. Then, we combine it with a backward Euler time-discretization and prove stability and error estimates. Finally, numerical results assessing the performance of the method are reported.

1. INTRODUCTION

The main goal of this paper is to analyze a numerical method to solve a transient eddy current axisymmetric problem. We consider the case of a coil supplied with a source current generating a magnetic field which induces eddy currents in a nearby workpiece. This classical model appears in many physical phenomena such as induction heating, electromagnetic stirring, magnetohydrodynamics or electromagnetic forming. In each case the induced currents in the workpiece have different roles (moving a fluid, heating or deforming the workpiece, etc); see for instance [1, 3, 8, 12, 16].

The cylindrical symmetry allows stating the eddy current problem in terms of the azimuthal component of a magnetic vector potential defined in a meridional section of the domain (see, for instance, [4]). We consider transient problems and assume a more general Ohm's law including velocity terms, which can be relevant in some industrial applications. As a consequence, we obtain a degenerate parabolic problem including convective terms which introduce interesting aspects in its mathematical and numerical analysis.

2000 *Mathematics Subject Classification.* Primary 78M10, 65N30.

Key words and phrases. Computational electromagnetism, eddy current problem, transient electromagnetics, finite elements, degenerate parabolic problem.

The first and the fourth author were partially supported by Xunta de Galicia under research project PGIDIT06PXIB207052PR by Ministerio de Ciencia e Innovación (Spain) under research projects Consolider MATHEMATICA CSD2006-00032 and MTM2008-02483.

The second author was supported by a MECESUP fellowship (Chile).

The third author was partially supported by FONDAP and BASAL projects CMM, Universidad de Chile (Chile) and Xunta de Galicia project PGIDIT06PXIB207052PR (Spain).

From a mathematical point of view, we cannot use the classical theory for abstract parabolic problems (see, for instance, [9]) because our formulation is degenerate. More precisely, the term involving the time derivative appears only in a part of the domain. Thus, in order to prove well-posedness, we resort to the theory for degenerate evolution problems proposed in [19]. On the other hand, the velocity term in the Ohm's law introduces a non-symmetric term which destroys the elliptic character of the bilinear form associated with the parabolic problem. However, we prove that a Gårding-like inequality holds, which allows us to use the theory from [19] by means of an exponential shift.

For the numerical solution of the problem, we discretize first in space by finite elements. This leads to a singular differential algebraic system (see [6]) which is proved to be well posed. We prove error estimates for this semi-discrete approximation. To do this, we adapt the classical theory (see [9]) to the degenerate character of the parabolic problem and the fact that the bilinear form is no longer elliptic. Then, we combine the finite element discretization with a backward Euler time-discretization. We prove error estimates for this fully discretized scheme by adapting once more the classical theory to the non-elliptic character of the bilinear form. Because of this, the error estimates are valid provided the time step is sufficiently small with respect to the physical data of the problem.

The outline of the paper is as follows: In Section 2, we describe the transient eddy current model and introduce a magnetic vector potential formulation under axisymmetric assumptions. In Section 3, we state the weak formulation and prove its well-posedness. In Section 4, we introduce the finite element space discretization and prove error estimates. In Section 5, we propose a backward Euler scheme for time discretization and prove error estimates for the fully discretized problem. Finally, in Section 6, we report some numerical tests which allow us to asses the performance of the proposed method.

2. Statement of the problem

We are interested in computing the eddy currents induced in a cylindrical workpiece by a nearby helical coil (see Figure 1 for possible configurations). The material on the workpiece is allowed to move, although without changing its domain.

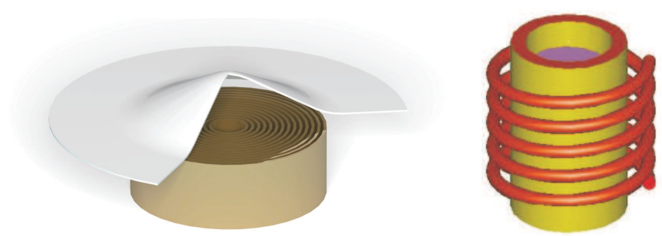

Figure 1. Sketch of the 3D-domain in some industrial applications.

In order to have a domain with cylindrical symmetry, we replace the coil by several superimposed rings with toroidal geometry. On the other hand, to solve the electromagnetic model in a bounded domain, we introduce a sufficiently large three dimensional cylinder $\widetilde{\Omega}$ of radius R and height L containing the coil and the workpiece.

Because of the cylindrical symmetry, we can work on a meridional section of $\widetilde{\Omega}$, which we denote by Ω. Let $\Omega_S := \Omega_1 \cup \cdots \cup \Omega_m$, where Ω_k ($k = 1, \ldots, m$) are the meridional sections of the turns of the coil. Let Ω_0 be the corresponding section of the workpiece and $\Omega_A := \Omega \setminus (\overline{\Omega}_S \cup \overline{\Omega}_0)$ the section of the domain occupied by the air. Let Γ_0 be the intersection between $\partial\Omega$ and the symmetry axis ($r = 0$) and $\Gamma_D := \partial\Omega \setminus \Gamma_0$ (see Figure 2).

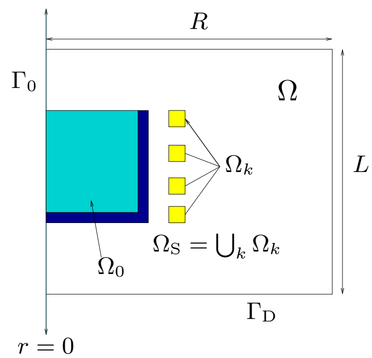

FIGURE 2. Sketch of the meridional section.

We will use standard notation:

- $\boldsymbol{E}$ is the electric field,
- $\boldsymbol{B}$ is the magnetic induction,
- $\boldsymbol{H}$ is the magnetic field,
- $\boldsymbol{J}$ is the current density,
- μ is the magnetic permeability,
- σ is the electric conductivity.

The physical parameters are supposed to satisfy:

$$0 < \underline{\mu} \leq \mu \leq \overline{\mu}, \tag{2.1}$$

$$0 < \underline{\sigma} \leq \sigma \leq \overline{\sigma} \quad \text{in conductors}, \tag{2.2}$$

$$\sigma = 0 \quad \text{in dielectrics}. \tag{2.3}$$

These parameters are assumed not to vary with time. This implies that the part of the workpiece subjected to motion has to be homogeneous (i.e., the parameters σ and μ are assumed to be constant on that part).

In this kind of problem, the electric displacement can be neglected in Ampère's law leading to the so called eddy current model:

$$\mathbf{curl}\, \boldsymbol{H} = \boldsymbol{J}, \tag{2.4}$$

$$\frac{\partial \boldsymbol{B}}{\partial t} + \mathbf{curl}\, \boldsymbol{E} = \boldsymbol{0}, \tag{2.5}$$

$$\operatorname{div} \boldsymbol{B} = 0. \tag{2.6}$$

This system must be completed with the following relations:

$$\boldsymbol{B} = \mu \boldsymbol{H}, \tag{2.7}$$

and

$$\boldsymbol{J} = \begin{cases} \sigma\boldsymbol{E} + \sigma\boldsymbol{v}\times\boldsymbol{B} & \text{in the workpiece,} \\ \boldsymbol{J}_{\mathrm{S}} & \text{in the coil (data),} \\ \boldsymbol{0} & \text{in the air.} \end{cases} \tag{2.8}$$

The vector field $\boldsymbol{v}$ in (2.8) represents the velocity of the material in the workpiece, which in the present analysis is taken as a data. The current density is taken as data in the coil ($\boldsymbol{J}_{\mathrm{S}}$) and unknown in the workpiece Ω_0. In the latter, $\boldsymbol{J}$ results from the eddy currents ($\sigma\boldsymbol{E}$) and the currents due to the motion of the workpiece ($\sigma\boldsymbol{v}\times\boldsymbol{B}$).

We assume that all the physical quantities are independent of the angular coordinate θ and that the current density field has only azimuthal non-zero component, i.e.,

$$\boldsymbol{J}(r,\theta,z) = J(r,z)\boldsymbol{e}_\theta. \tag{2.9}$$

We also assume that the velocity has only meridional components, $\boldsymbol{v} = v_r(r,z)\boldsymbol{e}_r + v_z(r,z)\boldsymbol{e}_z$, as corresponds to an axisymmetric problem.

Proceeding as in [4], it can be shown that

$$\boldsymbol{H}(r,\theta,z) = H_r(r,z)\boldsymbol{e}_r + H_z(r,z)\boldsymbol{e}_z, \tag{2.10}$$

$$\boldsymbol{B}(r,\theta,z) = B_r(r,z)\boldsymbol{e}_r + B_z(r,z)\boldsymbol{e}_z, \tag{2.11}$$

$$\boldsymbol{E}(r,\theta,z) = E(r,z)\boldsymbol{e}_\theta \qquad \text{in the workpiece.} \tag{2.12}$$

Moreover, from (2.6), the arguments in [4] allow us to introduce a vector potential $\boldsymbol{A}$ for $\boldsymbol{B}$,

$$\boldsymbol{B} = \mathbf{curl}\,\boldsymbol{A}, \tag{2.13}$$

of the form

$$\boldsymbol{A}(r,\theta,z) = A(r,z)\boldsymbol{e}_\theta. \tag{2.14}$$

Using (2.13) in (2.5), we obtain $\mathbf{curl}\left(\frac{\partial\boldsymbol{A}}{\partial t} + \boldsymbol{E}\right) = \boldsymbol{0}$ in the workpiece. On the other hand, using (2.12) and (2.14), from the expression of the **curl** in cylindrical coordinates we obtain

$$\frac{1}{r}\left\{\frac{\partial}{\partial z}\left[r\left(\frac{\partial A}{\partial t} + E\right)\right]\boldsymbol{e}_r + \frac{\partial}{\partial r}\left[r\left(\frac{\partial A}{\partial t} + E\right)\right]\boldsymbol{e}_z\right\} = \boldsymbol{0}.$$

Hence we deduce that

$$r\left(\frac{\partial A}{\partial t} + E\right) = C,$$

with C an arbitrary constant. This constant has to vanish in most cases of interest. In fact, typically $\partial\Omega_0$ intersects Γ_0 in a set with a non vanishing 1D measure (for instance in the cases depicted in Figure 1). In such a case, it is immediate to show that for $\frac{\partial A}{\partial t} + E = \frac{C}{r}$ to be square integrable in the workpiece, C has to vanish. Hence, we write

$$\frac{\partial A}{\partial t} + E = 0 \qquad \text{in } \Omega_0.$$

Therefore, substituting this expression in (2.8), we obtain

$$
J\boldsymbol{e}_\theta = \begin{cases} -\sigma \dfrac{\partial A}{\partial t}\boldsymbol{e}_\theta + \sigma \boldsymbol{v} \times \mathbf{curl}\,(A\boldsymbol{e}_\theta) & \text{in } \Omega_0, \\ J_{\mathrm{S}}\boldsymbol{e}_\theta & \text{in } \Omega_{\mathrm{S}}, \\ \mathbf{0} & \text{in } \Omega_{\mathrm{A}}. \end{cases} \tag{2.15}
$$

On the other hand, using (2.4), (2.7), (2.9), (2.13), and (2.14), we have

$$
\mathbf{curl}\left[\frac{1}{\mu}\,\mathbf{curl}\,(A\boldsymbol{e}_\theta)\right] = J\boldsymbol{e}_\theta,
$$

Thus, we are led to the following parabolic-elliptic problem:

$$
\begin{cases} \sigma \dfrac{\partial A}{\partial t}\boldsymbol{e}_\theta + \mathbf{curl}\left[\dfrac{1}{\mu}\,\mathbf{curl}\,(A\boldsymbol{e}_\theta)\right] - \boldsymbol{v} \times \mathbf{curl}\,(A\boldsymbol{e}_\theta) = \mathbf{0} & \text{in } \Omega_0, \\ \mathbf{curl}\left[\dfrac{1}{\mu}\,\mathbf{curl}\,(A\boldsymbol{e}_\theta)\right] = J_{\mathrm{S}}\boldsymbol{e}_\theta & \text{in } \Omega_{\mathrm{S}}, \\ \mathbf{curl}\left[\dfrac{1}{\mu}\,\mathbf{curl}\,(A\boldsymbol{e}_\theta)\right] = \mathbf{0} & \text{in } \Omega_{\mathrm{A}}. \end{cases} \tag{2.16}
$$

Finally we impose homogeneous Dirichlet boundary conditions for the vector potential A on Γ_{D}, which makes sense provided Γ_{D} has been chosen sufficiently far away from Ω_0 and Ω_{S}.

3. Weak Formulation

In this section we will obtain a weak formulation of the electromagnetic model given above and prove its well-posedness. Let $L^2_r(\Omega)$ be the weighted Lebesgue space of all measurable functions Z defined in Ω such that

$$
\|Z\|^2_{L^2_r(\Omega)} := \int_\Omega |Z|^2\, r\, dr\, dz < \infty.
$$

Clearly, $Z\boldsymbol{e}_\theta \in L^2(\widetilde{\Omega})^3$ if and only if $Z \in L^2_r(\Omega)$. We will use $(\cdot,\cdot)_{L^2_r(\Omega)}$ to denote the corresponding inner product. The weighted Sobolev space $H^k_r(\Omega)$ consists of all functions in $L^2_r(\Omega)$ whose derivatives up to the order k are also in $L^2_r(\Omega)$. We define the norms and seminorms in the standard way; in particular

$$
|Z|^2_{H^1_r(\Omega)} := \int_\Omega \left(|\partial_r Z|^2 + |\partial_z Z|^2\right) r\, dr\, dz.
$$

Let $L^2_{1/r}(\Omega)$ be the weighted Lebesgue space of all measurable functions Z defined in Ω such that

$$
\|Z\|^2_{L^2_{1/r}(\Omega)} := \int_\Omega \frac{|Z|^2}{r}\, dr\, dz < \infty.
$$

Let us define the Hilbert space

$$
\widetilde{H}^1_r(\Omega) := \left\{ Z \in H^1_r(\Omega) :\ Z \in L^2_{1/r}(\Omega) \right\},
$$

with the norm

$$
\|Z\|_{\widetilde{H}^1_r(\Omega)} := \left[\|Z\|^2_{H^1_r(\Omega)} + \|Z\|^2_{L^2_{1/r}(\Omega)}\right]^{1/2}.
$$

It is well known (see [5, 13]) that $Z\boldsymbol{e}_\theta \in H^1(\widetilde{\Omega})^3$ if and only if $Z \in \widetilde{H}^1_r(\Omega)$. Finally, let

$$
\mathcal{V} := \{Z \in \widetilde{H}^1_r(\Omega) :\ Z = 0 \text{ on } \Gamma_D\}
$$

and

$$\mathcal{V}_0 := \widetilde{H}^1_r(\Omega_0).$$

Regarding the data of our problem we assume that $\boldsymbol{v}$ is bounded, i.e.,

$$|\boldsymbol{v}(t,r,z)| \le \|\boldsymbol{v}\|_\infty \qquad \forall t \in [0,T] \quad \forall (r,z) \in \Omega_0,$$

and $J_{\mathrm{S}} \in L^2(0,T;L^2_r(\Omega_{\mathrm{S}}))$.

By testing (2.16) with $Z\boldsymbol{e}_\theta$, $Z \in \mathcal{V}$, we obtain

$$\int_{\Omega_0} \sigma \partial_t A Z\, r\,dr\,dz + \int_\Omega \frac{1}{\mu} \mathbf{curl}\,(A\boldsymbol{e}_\theta)\cdot \mathbf{curl}\,(Z\boldsymbol{e}_\theta)\, r\,dr\,dz - \int_{\Omega_0} \sigma \boldsymbol{v} \times \mathbf{curl}\,(A\boldsymbol{e}_\theta)\cdot (Z\boldsymbol{e}_\theta)\, r\,dr\,dz = \int_{\Omega_{\mathrm{S}}} J_{\mathrm{S}} Z\, r\,dr\,dz. \tag{3.1}$$

We have to add to this equation an initial condition $A(0) = A^0$ in Ω_0.

We define the bilinear forms

$$\widetilde{a}(Y,Z) := \int_\Omega \frac{1}{\mu} \mathbf{curl}\,(Y\boldsymbol{e}_\theta)\cdot \mathbf{curl}\,(Z\boldsymbol{e}_\theta)\, r\,dr\,dz, \quad Y, Z \in \mathcal{V},$$

$$c(t,Y,Z) := -\int_{\Omega_0} \sigma \boldsymbol{v}(t) \times \mathbf{curl}\,(Y\boldsymbol{e}_\theta)\cdot (Z\boldsymbol{e}_\theta)\, r\,dr\,dz, \quad Y, Z \in \mathcal{V},$$

and

$$a(t,Y,Z) := \widetilde{a}(Y,Z) + c(t,Y,Z). \tag{3.2}$$

Let $\mathcal{V}_0'$ be the dual space of $\mathcal{V}_0$ with respect to the pivot space $L^2_r(\Omega_0)$ with measure $\sigma\, r\,dr\,dz$ (which according to (2.2) is topologically equivalent to $L^2_r(\Omega_0)$ with measure $r\,dr\,dz$). Let us define the space

$$\mathcal{W}_0 := \left\{ Y \in L^2(0,T;\mathcal{V}) : \ \partial_t Y \in L^2(0,T;\mathcal{V}_0') \right\}.$$

Thus, from (3.1), we arrive at the following problem:

Problem 3.1. *Find $A \in \mathcal{W}_0$ such that*

$$\begin{cases} \langle \partial_t A, Z\rangle_{\mathcal{V}_0' \times \mathcal{V}_0} + a(t,A,Z) = (J_{\mathrm{S}}, Z)_{L^2_r(\Omega_{\mathrm{S}})} \quad \forall Z \in \mathcal{V}, \\ A(0)|_{\Omega_0} = A^0. \end{cases}$$

The initial data A^0 is taken in $L^2_r(\Omega_0)$. Let us remark that this initial condition makes sense because $\mathcal{W}_0 \hookrightarrow \mathcal{C}^0(0,T;L^2_r(\Omega_0))$ (see [18], for instance).

It is simple to show that $\widetilde{a}$ is $\mathcal{V}$-elliptic (see [10, Prop. 2.1]); namely, there exists $\alpha > 0$ such that

$$\widetilde{a}(Z,Z) \ge \alpha \|Z\|^2_{\widetilde{H}^1_r(\Omega)} \quad \forall Z \in \mathcal{V}. \tag{3.3}$$

Our next step is to prove a Gårding-like inequality for the bilinear form a.

Lemma 3.1. *Let $\lambda^* := \|\boldsymbol{v}\|^2_\infty \overline{\sigma}/\alpha$. For all $\lambda \ge \lambda^*$ and for all $Z \in \mathcal{V}$,*

$$a(t,Z,Z) + \lambda\, (\sigma Z, Z)_{L^2_r(\Omega_0)} \ge \frac{\alpha}{2} \|Z\|^2_{\widetilde{H}^1_r(\Omega)} \quad \forall t \in [0,T].$$

Proof. First, we estimate the term $c(t,Z,Z)$. With this aim, we use the expression of $\mathbf{curl}\,(Z\boldsymbol{e}_\theta)$ in cylindrical coordinates to write

$$c(t,Z,Z) = \int_{\Omega_0} \sigma v_r \frac{1}{r} \frac{\partial (rZ)}{\partial r} Z\, r\,dr\,dz - \int_{\Omega_0} \sigma v_z \frac{\partial Z}{\partial z} Z\, r\,dr\,dz.$$

Then, we use a weighted Cauchy-Schwartz inequality to obtain for all $\epsilon > 0$ and all $t \in [0,T]$

$$\left|\int_{\Omega_0} \sigma v_r \frac{1}{r}\frac{\partial(rZ)}{\partial r} Z\, r\, dr\, dz\right| \leq \epsilon \left[\|\partial_r Z\|^2_{L^2_r(\Omega_0)} + \|Z\|^2_{L^2_{1/r}(\Omega_0)}\right] + \frac{\overline{\sigma}\|v_r\|^2_\infty}{4\epsilon}\|\sigma^{1/2}Z\|^2_{L^2_r(\Omega_0)}$$

and

$$\left|\int_{\Omega_0} \sigma v_z \frac{\partial Z}{\partial z} Z\, r\, dr\, dz\right| \leq \epsilon\|\partial_z Z\|^2_{L^2_r(\Omega_0)} + \frac{\|v_z\|^2_\infty \overline{\sigma}}{4\epsilon}\|\sigma^{1/2}Z\|^2_{L^2_r(\Omega_0)}.$$

Hence

$$|c(t,Z,Z)| \leq 2\epsilon\|Z\|^2_{\widetilde{H}^1_r(\Omega)} + \frac{\|\boldsymbol{v}\|^2_\infty \overline{\sigma}}{4\epsilon}\|\sigma^{1/2}Z\|^2_{L^2_r(\Omega_0)}.$$

Therefore, from this inequality and (3.3),

$$\begin{aligned} a(t,Z,Z) + \lambda\,(\sigma Z, Z)_{L^2_r(\Omega_0)} &= \widetilde{a}(Z,Z) + c(t,Z,Z) + \lambda\|\sigma^{1/2}Z\|^2_{L^2_r(\Omega_0)} \\ &\geq (\alpha - 2\epsilon)\|Z\|^2_{\widetilde{H}^1_r(\Omega)} + \left(\lambda - \frac{\|\boldsymbol{v}\|^2_\infty\overline{\sigma}}{4\epsilon}\right)\|\sigma^{1/2}Z\|^2_{L^2_r(\Omega_0)}. \end{aligned}$$

Thus, the lemma holds by taking $\epsilon = \alpha/4$. $\square$

Now, we are a position to prove the main theorem of this section. In its proof and throughout the paper C will denote a constant not necessarily the same at each occurrence.

Theorem 3.2. *Problem 3.1 has a unique solution $A \in \mathcal{W}_0$ and there exists a positive constant C independent of the data of the problem, J_{S} and A^0, such that*

$$\|A\|_{L^2(0,T;\widetilde{H}^1_r(\Omega))} \leq C\left[\|J_{\mathrm{S}}\|^2_{L^2(0,T;L^2_r(\Omega_{\mathrm{S}}))} + \|A^0\|^2_{L^2_r(\Omega_0)}\right]^{1/2}.$$

Proof. Let $\lambda \geq \lambda^*$, with λ^* as in Lemma 3.1, and $\widehat{A} := e^{-\lambda t}A$. Then, A is a solution of Problem 3.1 if and only if $\widehat{A} \in \mathcal{W}_0$ is a solution of the following problem:

$$\begin{cases} \langle \partial_t \widehat{A}, Z\rangle_{\mathcal{V}_0'\times\mathcal{V}_0} + \widehat{a}(t,\widehat{A},Z) = (J_{\mathrm{S}}, Z)_{L^2_r(\Omega_{\mathrm{S}})} \quad \forall Z \in \mathcal{V}, \\ \widehat{A}(0)|_{\Omega_0} = A^0, \end{cases} \tag{3.4}$$

where

$$\widehat{a}(t,\widehat{A},Z) := a(t,\widehat{A},Z) + \lambda(\sigma\widehat{A},Z)_{L^2_r(\Omega_0)}.$$

Lemma 3.1 guarantees that $\widehat{a}(t,\widehat{A},\widehat{A}) \geq \frac{\alpha}{2}\|\widehat{A}\|^2_{\widetilde{H}^1_r(\Omega)}$. Hence, the existence of a unique solution of problem (3.4) follows from [19, Theorem 2] (see also [20]).

Next, testing the first equation of (3.4) with $Z = \widehat{A}$ and integrating with respect to time, we obtain (see [15, Prop. 1.2])

$$\frac{1}{2}\int_0^T \frac{d}{dt}(\sigma\widehat{A},\widehat{A})_{L^2_r(\Omega_0)}\,dt + \int_0^T \widehat{a}(t,\widehat{A},\widehat{A})\,dt = \int_0^T (J_{\mathrm{S}},\widehat{A})_{L^2_r(\Omega_{\mathrm{S}})}\,dt.$$

Consequently,

$$\begin{aligned} \|\sigma^{1/2}\widehat{A}(T)\|^2_{L^2_r(\Omega_0)} - \|\sigma^{1/2}\widehat{A}(0)\|^2_{L^2_r(\Omega_0)} + \frac{\alpha}{2}\|\widehat{A}\|^2_{L^2(0,T;\widetilde{H}^1_r(\Omega))} \\ \leq \|J_{\mathrm{S}}\|_{L^2(0,T;L^2_r(\Omega_{\mathrm{S}}))}\|\widehat{A}\|_{L^2(0,T;\widetilde{H}^1_r(\Omega))} \end{aligned}$$

and hence

$$\|\widehat{A}\|^2_{L^2(0,T;\widetilde{H}^1_r(\Omega))} \leq C\left[\|J_{\mathrm{S}}\|^2_{L^2(0,T;L^2_r(\Omega_{\mathrm{S}}))} + \|\widehat{A}(0)\|^2_{L^2_r(\Omega_0)}\right].$$

Therefore, by using that $A = e^{\lambda t}\widehat{A}$ and the initial condition of problem (3.4), we conclude the proof. $\square$

4. Semi-discrete problem

From now on we assume that Ω_0 is a polygonal domain. Let $\{\mathcal{T}_h\}_{h>0}$ be a regular family of triangulations of Ω such that each element $T \in \mathcal{T}_h$ is contained either in $\overline{\Omega_0}$ or in $\overline{\Omega \setminus \Omega_0}$. Therefore

$$\mathcal{T}_h^0 := \{T \in \mathcal{T}_h : \ T \subset \Omega_0\}$$

is a triangulation of Ω_0. The parameter h stands for the mesh-size. Let

$$\mathcal{V}_h := \{A_h \in \mathcal{V} : \ A_h|_T \in \mathbb{P}_1 \ \forall T \in \mathcal{T}_h\}$$

and

$$\mathcal{V}_h^0 := \left\{A_h \in \mathcal{V}_0 : \ A_h|_T \in \mathbb{P}_1 \ \forall T \in \mathcal{T}_h^0\right\},$$

where

$$\mathbb{P}_1 := \{p(r,z) = c_0 + c_1 r + c_2 z, \ c_0, c_1, c_2 \in \mathbb{R}\}.$$

We consider the Lagrange interpolation operator $\mathcal{I}_h \in \mathcal{L}(H^2_r(\Omega), \mathcal{V}_h)$. The proof of the following estimate can be found in [13, Prop. 6.1].

Theorem 4.1. *There exists a positive constant C, independent of h, such that for all $Z \in \mathcal{V} \cap H^2_r(\Omega)$*

$$\|Z - \mathcal{I}_h Z\|_{\widetilde{H}^1_r(\Omega)} \leq Ch\|Z\|_{H^2_r(\Omega)}.$$

By using this finite element space we are led to the following discretization of Problem 3.1:

Problem 4.1. *Find $A_h \in H^1(0,T;\mathcal{V}_h)$ such that*

$$\begin{cases} (\sigma\partial_t A_h, Z_h)_{L^2_r(\Omega_0)} + a(t, A_h, Z_h) = (J_{\mathrm{S}}, Z_h)_{L^2_r(\Omega_{\mathrm{S}})} \quad \forall Z_h \in \mathcal{V}_h, \\ A_h(0)|_{\Omega_0} = A_h^0. \end{cases}$$

The initial data A_h^0 has to belong to $\mathcal{V}_h^0$ and should be a reasonable approximation to A^0. Provided the latter is sufficiently smooth, a natural choice is $A_h^0 = \mathcal{I}_h A^0$, for instance. Moreover, because of the degenerate character of the problem, for its solution to lie in $H^1(0,T;\mathcal{V}_h)$, we will have to assume additional regularity in time of the source current. In fact, from now on we assume

$$J_{\mathrm{S}} \in H^1(0,T;L^2_r(\Omega_{\mathrm{S}})). \tag{4.1}$$

We note that Problem 4.1 is a linear system of ordinary differential-algebraic equations. To prove that this system has a unique solution, we will write it in matrix form.

With this aim, let $\{\phi_1, \ldots, \phi_N\}$ be the nodal basis of $\mathcal{V}_h$ ordered in such a way that $\{\phi_1|_{\Omega_0}, \ldots, \phi_M|_{\Omega_0}\}$ $(M < N)$ is a basis of $\mathcal{V}_h^0$. For all $t \in [0,T]$, a solution A_h to Problem 4.1 can be written as follows:

$$A_h(t,r,z) = \sum_{i=1}^N A_i(t)\phi_i(r,z).$$

Analogously we write

$$A_h^0 = \sum_{i=1}^{M} A_i^0 \phi_i|_{\Omega_0}.$$

For all $t \in [0,T]$, we set $\boldsymbol{\mathcal{A}}(t) := (A_i(t))_{1\le i\le N}$ and $\boldsymbol{\mathcal{F}}(t) := \left((J_{\mathrm{S}}(t), \phi_i)_{L_r^2(\Omega_{\mathrm{S}})}\right)_{1\le i\le N}$. We also set $\boldsymbol{\mathcal{A}}^0 := \left(A_i^0\right)_{1\le i\le M}$.

We introduce the matrices $\boldsymbol{\mathcal{K}}(t) := (K_{ij}(t))_{1\le i,j\le N}$ and $\boldsymbol{\mathcal{M}} := (M_{ij})_{1\le i,j\le N}$, with

$$K_{ij}(t) := a(t, \phi_i, \phi_j), \qquad M_{ij} := (\sigma\phi_i, \phi_j)_{L_r^2(\Omega_0)}, \qquad 1 \le i,j \le N.$$

Since the initial condition in Problem 4.1 involves only the components of $A_h(0)$ which correspond to the nodes in the conducting domain Ω_0, we decompose $\boldsymbol{\mathcal{A}}(t)$ as follows:

$$\boldsymbol{\mathcal{A}}(t) = \begin{bmatrix} \boldsymbol{\mathcal{A}}_{\mathrm{C}}(t) \\ \boldsymbol{\mathcal{A}}_{\mathrm{D}}(t) \end{bmatrix},$$

with $\boldsymbol{\mathcal{A}}_{\mathrm{C}}(t) = (A_i(t))_{1\le i\le M}$ and $\boldsymbol{\mathcal{A}}_{\mathrm{D}}(t) = (A_i(t))_{M+1\le i\le N}$. Therefore, Problem 4.1 can be written in the following form:

$$\begin{cases} \boldsymbol{\mathcal{M}}\boldsymbol{\mathcal{A}}'(t) + \boldsymbol{\mathcal{K}}(t)\boldsymbol{\mathcal{A}}(t) = \boldsymbol{\mathcal{F}}(t), \\ \qquad\qquad\qquad \boldsymbol{\mathcal{A}}_{\mathrm{C}}(0) = \boldsymbol{\mathcal{A}}^0. \end{cases}$$

This is a degenerate problem, because the matrix $\boldsymbol{\mathcal{M}}$ is singular. Hence, to prove its well-posedness, we write it in block matrix form:

$$\begin{cases} \begin{bmatrix} \boldsymbol{\mathcal{M}}_{\mathrm{CC}} & \mathbf{0} \\ \mathbf{0} & \mathbf{0} \end{bmatrix} \begin{bmatrix} \boldsymbol{\mathcal{A}}_{\mathrm{C}}'(t) \\ \boldsymbol{\mathcal{A}}_{\mathrm{D}}'(t) \end{bmatrix} + \begin{bmatrix} \boldsymbol{\mathcal{K}}_{\mathrm{CC}}(t) & \boldsymbol{\mathcal{K}}_{\mathrm{CD}} \\ \boldsymbol{\mathcal{K}}_{\mathrm{DC}} & \boldsymbol{\mathcal{K}}_{\mathrm{DD}} \end{bmatrix} \begin{bmatrix} \boldsymbol{\mathcal{A}}_{\mathrm{C}}(t) \\ \boldsymbol{\mathcal{A}}_{\mathrm{D}}(t) \end{bmatrix} = \begin{bmatrix} \mathbf{0} \\ \boldsymbol{\mathcal{F}}_{\mathrm{D}}(t) \end{bmatrix}, \\ \qquad\qquad\qquad\qquad\qquad\qquad \boldsymbol{\mathcal{A}}_{\mathrm{C}}(0) = \boldsymbol{\mathcal{A}}^0. \end{cases}$$

Notice that only $\boldsymbol{\mathcal{K}}_{\mathrm{CC}}$ depends on t. Indeed, since $\boldsymbol{v}$ vanishes in $\overline{\Omega} \setminus \overline{\Omega}_0$, we have that $c(t, \phi_i, \phi_j) \neq 0$ only if ϕ_i and ϕ_j correspond to nodes in $\overline{\Omega}_0$. Moreover, from the ellipticity of $\widetilde{a}$, $\boldsymbol{\mathcal{K}}_{\mathrm{DD}}$ is positive definite and we can write

$$\boldsymbol{\mathcal{A}}_{\mathrm{D}}(t) = \boldsymbol{\mathcal{K}}_{\mathrm{DD}}^{-1}\left[-\boldsymbol{\mathcal{K}}_{\mathrm{DC}}\boldsymbol{\mathcal{A}}_{\mathrm{C}}(t) + \boldsymbol{\mathcal{F}}_{\mathrm{D}}(t)\right]. \tag{4.2}$$

Hence,

$$\begin{cases} \boldsymbol{\mathcal{M}}_{\mathrm{CC}}\boldsymbol{\mathcal{A}}_{\mathrm{C}}'(t) = \left[-\boldsymbol{\mathcal{K}}_{\mathrm{CC}}(t) + \boldsymbol{\mathcal{K}}_{\mathrm{CD}}\boldsymbol{\mathcal{K}}_{\mathrm{DD}}^{-1}\boldsymbol{\mathcal{K}}_{\mathrm{DC}}\right]\boldsymbol{\mathcal{A}}_{\mathrm{C}}(t) - \boldsymbol{\mathcal{K}}_{\mathrm{CD}}\boldsymbol{\mathcal{K}}_{\mathrm{DD}}^{-1}\boldsymbol{\mathcal{F}}_{\mathrm{D}}(t), \\ \qquad \boldsymbol{\mathcal{A}}_{\mathrm{C}}(0) = \boldsymbol{\mathcal{A}}^0. \end{cases}$$

Since $\boldsymbol{\mathcal{M}}_{\mathrm{CC}}$ is also positive definite, this linear system of ordinary differential-algebraic equations has a unique solution. Moreover, $\boldsymbol{\mathcal{K}}_{\mathrm{CC}} \in L^2(0,T;\mathbb{R}^{M\times M})$ and consequently $\boldsymbol{\mathcal{A}}_{\mathrm{C}} \in H^1(0,T;\mathbb{R}^M)$. Finally, from the assumption (4.1), we obtain from (4.2) that $\boldsymbol{\mathcal{A}}_{\mathrm{D}} \in H^1(0,T;\mathbb{R}^{N-M})$. Thus, we have proved the following result:

Theorem 4.2. *Problem 4.1 is well-posed.*

In what follows we will prove error estimates for this semi-discrete problem. Since the bilinear form a is not elliptic due to the presence of the velocity terms, we use its elliptic part $\widetilde{a}$ to define an elliptic projector. In this context, we can find in [17] some alternatives.

Let us introduce $P_h \in \mathcal{L}(\mathcal{V}, \mathcal{V}_h)$ by

$$\widetilde{a}(P_h Y, Z_h) = \widetilde{a}(Y, Z_h) \qquad \forall Z_h \in \mathcal{V}_h, \quad Y \in \mathcal{V}.$$

Notice that, from Cea's lemma and Theorem 4.1, for all $Y \in H_r^2(\Omega) \cap \mathcal{V}$

$$\|Y - P_h Y\|_{\widetilde{H}_r^1(\Omega)} \leq C\|Y - \mathcal{I}_h Y\|_{\widetilde{H}_r^1(\Omega)} \leq Ch\|Y\|_{H_r^2(\Omega)}; \tag{4.3}$$

moreover, a standard duality argument leads to

$$\|Y - P_h Y\|_{L_r^2(\Omega)} \leq Ch^2\|Y\|_{H_r^2(\Omega)}. \tag{4.4}$$

Let A and A_h be the solutions to Problems 3.1 and 4.1, respectively. We write

$$A(t) - A_h(t) = \delta_h(t) + \rho_h(t),$$

where

$$\delta_h(t) := P_h A(t) - A_h(t) \qquad \text{and} \qquad \rho_h(t) := A(t) - P_h A(t).$$

Provided A is smooth enough, $\partial_t(P_h A) = P_h(\partial_t A)$ (cf [18, Theorem P.111]) and, consequently, we have from (4.4)

$$\|\partial_t \rho_h\|_{L_r^2(\Omega)} \leq Ch^2\|\partial_t A\|_{H_r^2(\Omega)}. \tag{4.5}$$

The following lemma is the basic tool to prove error estimates for the semi-discrete problem.

Lemma 4.3. *If $A \in H^1(0,T; H_r^2(\Omega) \cap \mathcal{V})$, then*

$$\|\delta_h\|_{\mathcal{C}^0(0,T;L_r^2(\Omega_0))} \leq C\left[\|\delta_h(0)\|_{L_r^2(\Omega_0)} + h\|A\|_{H^1(0,T;H_r^2(\Omega))}\right], \tag{4.6}$$

$$\|\delta_h\|_{L^2(0,T;\widetilde{H}_r^1(\Omega))} \leq C\left[\|\delta_h(0)\|_{L_r^2(\Omega_0)} + h\|A\|_{H^1(0,T;H_r^2(\Omega))}\right], \tag{4.7}$$

$$\|\partial_t\delta_h\|_{L^2(0,T;L_r^2(\Omega_0))} \leq C\left[\|\delta_h(0)\|_{\widetilde{H}_r^1(\Omega)} + h\|A\|_{H^1(0,T;H_r^2(\Omega))}\right]. \tag{4.8}$$

Proof. Testing Problems 3.1 and 4.1 with $Z_h \in \mathcal{V}_h \subset \mathcal{V}$ and subtracting, we obtain

$$(\sigma\partial_t(A - A_h), Z_h)_{L_r^2(\Omega_0)} + a(t, A - A_h, Z_h) = 0 \quad \forall Z_h \in \mathcal{V}_h,$$

where we have used that $\partial_t A \in L_r^2(\Omega_0)$ (because of the assumed regularity) to write the duality pairing as an inner product. Using that $A(t) - A_h(t) = \delta_h(t) + \rho_h(t)$ and (3.2), we have

$$(\sigma\partial_t\delta_h(t), Z_h)_{L_r^2(\Omega_0)} + a(\delta_h(t), Z_h) = -(\sigma\partial_t\rho_h(t), Z_h)_{L_r^2(\Omega_0)} - c(t, \rho_h(t), Z_h). \tag{4.9}$$

By setting $Z_h = \delta_h(t)$, we obtain

$$\begin{aligned}\frac{1}{2}\frac{d}{dt}(\sigma\delta_h(t), \delta_h(t))_{L_r^2(\Omega_0)} &+ a(\delta_h(t), \delta_h(t)) \\ &= -(\sigma\partial_t\rho_h(t), \delta_h(t))_{L_r^2(\Omega_0)} - c(t, \rho_h(t), \delta_h(t)).\end{aligned}$$

We use Lemma 3.1 and a weighted Cauchy-Schwartz inequality to write

$$\begin{aligned}\frac{1}{2}\frac{d}{dt}\|\sigma^{1/2}\delta_h(t)\|^2_{L_r^2(\Omega_0)} &+ \frac{\alpha}{2}\|\delta_h(t)\|^2_{\widetilde{H}_r^1(\Omega)} - \lambda^*\|\sigma^{1/2}\delta_h(t)\|^2_{L_r^2(\Omega_0)} \\ &\leq \frac{\alpha}{4}\|\delta_h(t)\|^2_{L_r^2(\Omega_0)} + C\left[\|\partial_t\rho_h(t)\|^2_{L_r^2(\Omega_0)} + \|\rho_h(t)\|^2_{\widetilde{H}_r^1(\Omega_0)}\right],\end{aligned}$$

with C depending only on $\|\boldsymbol{v}\|_\infty$, $\overline{\sigma}$, and α. Then,

$$\begin{aligned}\frac{d}{dt}\|\sigma^{1/2}\delta_h(t)\|^2_{L_r^2(\Omega_0)} &+ \frac{\alpha}{2}\|\delta_h(t)\|^2_{\widetilde{H}_r^1(\Omega)} \\ &\leq C\left[\|\sigma^{1/2}\delta_h(t)\|^2_{L_r^2(\Omega_0)} + \|\partial_t\rho_h(t)\|^2_{L_r^2(\Omega_0)} + \|\rho_h(t)\|^2_{\widetilde{H}_r^1(\Omega_0)}\right].\end{aligned} \tag{4.10}$$

The term involving $\|\delta_h(t)\|_{\widetilde{H}^1_r(\Omega)}$ can be dropped out and the inequality is preserved. Hence, using Gronwall inequality we obtain

$$\begin{aligned}\|\sigma^{1/2}\delta_h(t)\|^2_{L^2_r(\Omega_0)}\\ &\leq C\left[\|\sigma^{1/2}\delta_h(0)\|^2_{L^2_r(\Omega_0)} + \|\partial_t\rho_h\|^2_{L^2(0,T;L^2_r(\Omega))} + \|\rho_h\|^2_{L^2(0,T;\widetilde{H}^1_r(\Omega))}\right].\end{aligned}$$

Thus, (4.6) follows from (4.3), (4.5), and the last inequality.

To prove (4.7) we integrate (4.10) with respect to time to obtain

$$\begin{aligned}\|\sigma^{1/2}\delta_h(T)\|^2_{L^2_r(\Omega_0)} - \|\sigma^{1/2}\delta_h(0)\|^2_{L^2_r(\Omega_0)} + \frac{\alpha}{2}\int_0^T \|\delta_h(t)\|^2_{\widetilde{H}^1_r(\Omega)}\,dt\\ \leq C\int_0^T \left[\|\sigma^{1/2}\delta_h(t)\|^2_{L^2_r(\Omega_0)} + \|\partial_t\rho_h(t)\|^2_{L^2_r(\Omega_0)} + \|\rho_h(t)\|^2_{\widetilde{H}^1_r(\Omega_0)}\right]dt.\end{aligned}$$

Hence, (4.7) follows from (4.6), (4.3), and (4.5) again.

Finally, to prove (4.8), we set $Z_h = \partial_t\delta_h(t)$ in (4.9) to write

$$\begin{aligned}(\sigma\partial_t\delta_h(t), \partial_t\delta_h(t))_{L^2_r(\Omega_0)} + \widetilde{a}(\delta_h(t), \partial_t\delta_h(t))\\ = -(\sigma\partial_t\rho_h(t), \partial_t\delta_h(t))_{L^2_r(\Omega_0)} - c(t, \delta_h(t), \partial_t\delta_h(t)) - c(t, \rho_h(t), \partial_t\delta_h(t)).\end{aligned}$$

We estimate the right hand side above by using a weighted Cauchy-Schwartz inequality. Then, since $\widetilde{a}$ is symmetric, we have

$$\begin{aligned}\|\sigma^{1/2}\partial_t\delta_h(t)\|^2_{L^2_r(\Omega_0)} + \frac{1}{2}\frac{d}{dt}\widetilde{a}(\delta_h(t), \delta_h(t))\\ \leq \frac{1}{2}\|\sigma^{1/2}\partial_t\delta_h(t)\|^2_{L^2_r(\Omega_0)} + C\left[\|\partial_t\rho_h(t)\|^2_{L^2_r(\Omega_0)} + \|\delta_h(t)\|^2_{\widetilde{H}^1_r(\Omega_0)} + \|\rho_h(t)\|^2_{\widetilde{H}^1_r(\Omega_0)}\right].\end{aligned}$$

Next, we integrate in $[0, T]$ to obtain

$$\begin{aligned}\frac{1}{2}\int_0^T \|\sigma^{1/2}\partial_t\delta_h(t)\|^2_{L^2_r(\Omega_0)}\,dt + \frac{1}{2}\widetilde{a}(\delta_h(T), \delta_h(T)) - \frac{1}{2}\widetilde{a}(\delta_h(0), \delta_h(0))\\ \leq C\int_0^T \left[\|\partial_t\rho_h(t)\|^2_{L^2_r(\Omega_0)} + \|\delta_h(t)\|^2_{\widetilde{H}^1_r(\Omega_0)} + \|\rho_h(t)\|^2_{\widetilde{H}^1_r(\Omega_0)}\right]dt.\end{aligned}$$

Thus, (4.8) follows from the ellipticity and the continuity of $\widetilde{a}$, (4.3), and (4.5). □

Now we are in a position to prove error estimates for the computed vector potential A_h as well as for the approximations of the physical quantities of interest that can be derived from it. According to (2.13) and (2.14), we define

$$\boldsymbol{B}_h := \mathbf{curl}(A_h\boldsymbol{e}_\theta)$$

and, according to (2.9) and (2.15),

$$\boldsymbol{J}_h := -\sigma\frac{\partial A_h}{\partial t}\boldsymbol{e}_\theta + \sigma\boldsymbol{v}\times\boldsymbol{B}_h \qquad \text{in } \Omega_0.$$

The following error estimates hold true.

Theorem 4.4. *Let A and A_h be the solutions to Problems 3.1 and 4.1, respectively. Let $\boldsymbol{B}$ be defined by (2.13) and (2.14) and $\boldsymbol{J}$ by (2.9) and (2.15). Let $\boldsymbol{B}_h$ and $\boldsymbol{J}_h$ be* *defined as above. If $A \in H^1(0,T;H_r^2(\Omega)\cap\mathcal{V})$, then there exists a positive constant C independent of h and A such that*

$$\|A-A_h\|_{\mathcal{C}^0(0,T;L_r^2(\Omega_0))} \le C\left[\|A^0-A_h^0\|_{L_r^2(\Omega_0)} + h\|A\|_{H^1(0,T;H_r^2(\Omega))}\right], \tag{4.11}$$

$$\|\boldsymbol{B}-\boldsymbol{B}_h\|_{L^2(0,T;L_r^2(\Omega))} \le C\left[\|A^0-A_h^0\|_{L_r^2(\Omega_0)} + h\|A\|_{H^1(0,T;H_r^2(\Omega))}\right], \tag{4.12}$$

$$\|\boldsymbol{J}-\boldsymbol{J}_h\|_{L^2(0,T;L_r^2(\Omega_0))} \le C\left[\|A(0)-A_h(0)\|_{\widetilde{H}_r^1(\Omega)} + h\|A\|_{H^1(0,T;H_r^2(\Omega))}\right]. \tag{4.13}$$

Proof. We use that $A(t)-A_h(t)=\delta_h(t)+\rho_h(t)$, (4.6), and (4.4), to write

$$\|A-A_h\|_{\mathcal{C}^0(0,T;L_r^2(\Omega_0))} \le C\left[\|\delta_h(0)\|_{L_r^2(\Omega_0)} + h\|A\|_{H^1(0,T;H_r^2(\Omega))}\right]$$

and

$$\begin{aligned}\|\delta_h(0)\|_{L_r^2(\Omega_0)} &\le \|A(0)-A_h(0)\|_{L_r^2(\Omega_0)} + \|\rho_h(0)\|_{L_r^2(\Omega_0)}\\ &\le \|A^0-A_h^0\|_{L_r^2(\Omega_0)} + Ch^2\|A(0)\|_{H_r^2(\Omega)}.\end{aligned}$$

Then, (4.11) follows from these inequalities.

For the second estimate we use the definitions of $\boldsymbol{B}$ and $\boldsymbol{B}_h$ and the same arguments, combined now with (4.7) and (4.3), to write

$$\begin{aligned}\|\boldsymbol{B}-\boldsymbol{B}^h\|_{L^2(0,T;L_r^2(\Omega))} &\le \|\delta_h\|_{L^2(0,T;\widetilde{H}_r^1(\Omega))} + \|\rho_h\|_{L^2(0,T;\widetilde{H}_r^1(\Omega))}\\ &\le C\left[\|A^0-A_h^0\|_{L_r^2(\Omega_0)} + h\|A\|_{H^1(0,T;H_r^2(\Omega))}\right].\end{aligned}$$

This inequality is also used to prove (4.13), together with the following one which follows again from the same arguments, (4.8), (4.5), and (4.3):

$$\begin{aligned}\|\partial_t A-\partial_t A_h\|_{L^2(0,T;L_r^2(\Omega_0))} &\le \|\partial_t\delta_h\|_{L^2(0,T;L_r^2(\Omega_0))} + \|\partial_t\rho_h\|_{L^2(0,T;L_r^2(\Omega_0))}\\ &\le C\left[\|A(0)-A_h(0)\|_{\widetilde{H}_r^1(\Omega)} + h\|A\|_{H^1(0,T;H_r^2(\Omega))}\right].\end{aligned}$$

Thus, according to the definitions of $\boldsymbol{J}$ and $\boldsymbol{J}_h$, (4.13) follows from the last two inequalities and we conclude the proof. □

Notice that in the theorem above, (4.13) is not an actual a priori error estimate. In fact,

$$\|A(0)-A_h(0)\|^2_{\widetilde{H}_r^1(\Omega)} = \|A(0)-A_h(0)\|^2_{\widetilde{H}_r^1(\Omega_0)} + \|A(0)-A_h(0)\|^2_{H^1(0,T;\Omega\setminus\overline{\Omega}_0)}.$$

The first term on the right hand side above depends only on the initial data of both problems: $\|A(0)-A_h(0)\|_{\widetilde{H}_r^1(\Omega_0)} = \|A^0-A_h^0\|_{\widetilde{H}_r^1(\Omega_0)}$. Instead the second one depends on the solutions of Problems 3.1 and 4.1. In what follows we prove that if we choose the initial data of the semi-discrete problem as the Lagrange interpolant of A^0 (which is well defined under the smoothness assumptions of Theorem 4.4), then the second term can be also conveniently bounded.

Lemma 4.5. *If $A \in H^1(0,T;H_r^2(\Omega)\cap\mathcal{V})$ and $A_h^0=\mathcal{I}_h A^0$, then there exists a positive constant C independent of h such that*

$$\|A(0)-A_h(0)\|_{\widetilde{H}_r^1(\Omega)} \le Ch\|A(0)\|_{H_r^2(\Omega)}$$

Proof. By testing Problems 3.1 and 4.1 with $Z_h\in\mathcal{V}_h$ and subtracting we have

$$\int_{\Omega_0}\sigma\left(\partial_t A(t)-\partial_t A_h(t)\right)Z_h\, r\,dr\,dz + \widetilde{a}(A(t)-A_h(t),Z_h) + c(t,A(t)-A_h(t),Z_h)=0.$$

Hence, if $Z_h \in \mathcal{V}_h$ is such that $\operatorname{supp} Z_h \subset \Omega \setminus \Omega_0$, we obtain

$$\widetilde{a}(A(t) - A_h(t), Z_h) = 0 \qquad \text{a.e. } t \in [0, T].$$

Since $A_h \in H^1(0, T; \mathcal{V}_h)$ and we have assumed $A \in H^1(0, T; \mathcal{V})$, we have that $\widetilde{a}(A(t) - A_h(t), Z_h)$ is a continuous function of t in $[0, T]$. Therefore, for all $Z_h \in \mathcal{V}_h$ such that $\operatorname{supp} Z_h \subset \Omega \setminus \Omega_0$, we can write

$$\widetilde{a}(A(0) - A_h(0), Z_h) = 0.$$

Let $Z_h := A_h(0) - \mathcal{I}_h A(0) \in \mathcal{V}_h$. Notice that $\operatorname{supp} Z_h \subset \Omega \setminus \Omega_0$, because

$$Z_h|_{\Omega_0} = A_h(0)|_{\Omega_0} - \mathcal{I}_h A(0)|_{\Omega_0} = A_h^0 - \mathcal{I}_h A^0 = 0.$$

Then,

$$\widetilde{a}(A(0) - A_h(0), A(0) - A_h(0)) = \widetilde{a}(A(0) - A_h(0), A(0) - \mathcal{I}_h A(0)).$$

Therefore, since $\widetilde{a}$ is elliptic, using Theorem 4.1 we have

$$\begin{aligned}\alpha \|A(0) - A_h(0)\|^2_{\widetilde{H}^1_r(\Omega)} &\le \widetilde{a}(A(0) - A_h(0), A(0) - \mathcal{I}_h A(0)) \\ &\le \|A(0) - A_h(0)\|_{\widetilde{H}^1_r(\Omega)} Ch \|A(0)\|_{H^2_r(\Omega)}.\end{aligned}$$

Hence we conclude the lemma. □

Now we are in a position to conclude an $\mathcal{O}(h)$ order of convergence.

Corollary 4.6. *Under the assumptions of Theorem 4.4, if $A_h^0 = \mathcal{I}_h A^0$, then there exists a positive constant C independent of h and A such that*

$$\begin{aligned}\|A - A_h\|_{\mathcal{C}^0(0,T;L^2_r(\Omega_0))} &\le Ch\|A\|_{H^1(0,T;H^2_r(\Omega))}, \\ \|\boldsymbol{B} - \boldsymbol{B}_h\|_{L^2(0,T;L^2_r(\Omega))} &\le Ch\|A\|_{H^1(0,T;H^2_r(\Omega))}, \\ \|\boldsymbol{J} - \boldsymbol{J}_h\|_{L^2(0,T;L^2_r(\Omega_0))} &\le Ch\|A\|_{H^1(0,T;H^2_r(\Omega))}.\end{aligned}$$

Proof. It is an immediate consequence of Theorem 4.4, Lemma 4.5, and Theorem 4.1. □

5. Fully Discrete Problem

In this section we introduce a time discretization of Problem 4.1 by means of a backward Euler scheme and prove its stability and convergence. With this aim, we will adapt the standard theory for parabolic problems (see, for instance, [9]) taking into account that in our case the problem is degenerate and the bilinear form is non-elliptic.

We consider a uniform partition $\{t^k := k\Delta t,\ k = 0, \dots, N\}$ of $[0, T]$ with time step $\Delta t := \frac{T}{N}$. A fully discrete approximation of Problem 3.1 is defined as follows:

Problem 5.1. *Given $A_h^0 \in \mathcal{V}_h^0$, for $k = 1, \dots, N$ find $A_h^k \in \mathcal{V}_h$ such that*

$$\frac{1}{\Delta t}\left(\sigma A_h^k - \sigma A_h^{k-1}, Z_h\right)_{L^2_r(\Omega_0)} + a(t^k, A_h^k, Z_h) = \left(J_{\mathrm{S}}(t^k), Z_h\right)_{L^2_r(\Omega_{\mathrm{S}})} \quad \forall Z_h \in \mathcal{V}_h.$$

First we prove that this problem is well-posed, at least for Δt sufficiently small, by means of the following stability result.

Theorem 5.1. *Let λ^* be defined as in Lemma 3.1. If $\lambda^*\Delta t < 1/4$, then Problem 5.1 has a unique solution and there exists a positive constant C independent of h, Δt, and the data of the problem, A_h^0 and J_{S}, such that*

$$\max_{1\le k\le N} \|A_h^k\|^2_{L^2_r(\Omega_0)} + \Delta t \sum_{k=1}^N \|A_h^k\|^2_{\widetilde{H}^1_r(\Omega)} \le C\left[\|A_h^0\|^2_{L^2_r(\Omega_0)} + \Delta t\sum_{k=1}^N \|J_{\mathrm{S}}(t^k)\|^2_{L^2_r(\Omega_{\mathrm{S}})}\right].$$

Proof. We only have to prove the estimate, since it implies that the fully discrete problem has a unique solution. To do this, we test Problem 5.1 with $Z_h = A_h^k$ to write

$$\left(\sigma A_h^k - \sigma A_h^{k-1}, A_h^k\right)_{L^2_r(\Omega_0)} + \Delta t\, a(t^k, A_h^k, A_h^k) = \Delta t\left(J_{\mathrm{S}}(t^k), A_h^k\right)_{L^2_r(\Omega_{\mathrm{S}})}.$$

On the other hand, we note that

$$\begin{aligned} (5.1)\quad & 2\left(\sigma A_h^k - \sigma A_h^{k-1}, A_h^k\right)_{L^2_r(\Omega_0)} \\ &= \|\sigma^{1/2}A_h^k\|^2_{L^2_r(\Omega_0)} - \|\sigma^{1/2}A_h^{k-1}\|^2_{L^2_r(\Omega_0)} + \|\sigma^{1/2}A_h^k - \sigma^{1/2}A_h^{k-1}\|^2_{L^2_r(\Omega_0)}, \end{aligned}$$

whereas from Lemma 3.1 we have

$$a(t^k, A_h^k, A_h^k) \ge \frac{\alpha}{2}\|A_h^k\|^2_{\widetilde{H}^1_r(\Omega)} - \lambda^*\|\sigma^{1/2}A_h^k\|^2_{L^2_r(\Omega_0)}.$$

Substituting these last two relations into the first one and using a weighted Cauchy-Schwarz inequality, we obtain

$$\begin{aligned} &\|\sigma^{1/2}A_h^k\|^2_{L^2_r(\Omega_0)} - \|\sigma^{1/2}A_h^{k-1}\|^2_{L^2_r(\Omega_0)} + \|\sigma^{1/2}A_h^k - \sigma^{1/2}A_h^{k-1}\|^2_{L^2_r(\Omega_0)} \\ &+ \alpha\Delta t\|A_h^k\|^2_{\widetilde{H}^1_r(\Omega)} - 2\lambda^*\Delta t\|\sigma^{1/2}A_h^k\|^2_{L^2_r(\Omega_0)} \\ &\qquad\qquad \le \frac{2\Delta t}{\alpha}\|J_{\mathrm{S}}(t^k)\|^2_{L^2_r(\Omega)} + \frac{\alpha\Delta t}{2}\|A_h^k\|^2_{\widetilde{H}^1_r(\Omega)}. \end{aligned}$$

We add the above inequalities from $k=1$ to n and use the assumption $\lambda^*\Delta t \le 1/4$ to write

$$\begin{aligned} (5.2)\quad & \frac{1}{2}\|\sigma^{1/2}A_h^n\|^2_{L^2_r(\Omega_0)} + \frac{\alpha\Delta t}{2}\sum_{k=1}^n \|A_h^k\|^2_{\widetilde{H}^1_r(\Omega)} \\ &\le \|\sigma^{1/2}A_h^0\|^2_{L^2_r(\Omega_0)} + \frac{2\Delta t}{\alpha}\sum_{k=1}^n \|J_{\mathrm{S}}(t^k)\|^2_{L^2_r(\Omega)} + 2\lambda^*\Delta t\sum_{k=1}^{n-1}\|\sigma^{1/2}A_h^k\|^2_{L^2_r(\Omega_0)}. \end{aligned}$$

Hence, the discrete Gronwall lemma, (see, for instance, [14, Lemma 1.4.2]) yields

$$\|\sigma^{1/2}A_h^n\|^2_{L^2_r(\Omega_0)} \le C\left[\|A_h^0\|^2_{L^2_r(\Omega_0)} + \Delta t\sum_{k=1}^n \|J_{\mathrm{S}}(t^k)\|^2_{L^2_r(\Omega)}\right], \quad n = 1,\dots,N.$$

On the other hand, setting $n = N$ in (5.2) and using the previous inequality we obtain

$$\Delta t\sum_{k=1}^N \|A_h^k\|^2_{\widetilde{H}^1_r(\Omega)} \le C\left[\|A_h^0\|^2_{L^2_r(\Omega_0)} + \Delta t\sum_{k=1}^N \|J_{\mathrm{S}}(t^k)\|^2_{L^2_r(\Omega)}\right].$$

Thus we conclude the proof. □

Our next goal is to prove error estimates for the solution of the fully discrete problem. To do this we introduce some notation. Given $(\phi^0,\dots,\phi^N)\in\mathbb{R}^{N+1}$, we define the backward difference quotient

$$\bar\partial\phi^k := \frac{\phi^k-\phi^{k-1}}{\Delta t}, \qquad k=1,\dots,N.$$

For A and A_h^k being the solutions of Problems 3.1 and 5.1, respectively, if $A\in\mathcal{C}^0(0,T;\mathcal{V})$, we write

$$A(t^k)-A_h^k=\delta_h^k+\rho_h^k \qquad \text{in } \Omega.$$

with

$$\delta_h^k := P_hA(t^k)-A_h^k \qquad \text{and} \qquad \rho_h^k := A(t^k)-P_hA(t^k), \qquad k=1,\dots,N.$$

In the proofs that follow we will have to use $\bar\partial\rho_h^k$ and $\bar\partial\delta_h^k$, which for $k=1$ involves δ_h^0 and ρ_h^0, The latter is well defined in the whole Ω by the same expression as above. However, this is not the case for δ_h^0, since the domain of the data A_h^0 is just Ω_0. To define δ_h^0 in the whole domain Ω, we need to consider an extension of A_h^0 outside Ω_0. In principle any arbitrary extension could be used. We resort to the solution A_h of the semi-discrete problem for reasons that will be clear below. Let

$$\rho_h^0 := A(0)-P_hA(0) \qquad \text{and} \qquad \delta_h^0 := P_hA(0)-A_h(0),$$

where A_h is the solution to Problem 4.1. Then,

$$A^0-A_h^0=\delta_h^0+\rho_h^0 \qquad \text{in } \Omega_0.$$

.

Finally, provided $A\in\mathcal{C}^1(0,T;L^2_r(\Omega_0))$, we define the truncation errors:

$$\tau^k := \bar\partial A(t^k)-\partial_tA(t^k) \qquad \text{in } \Omega_0, \qquad k=1,\dots,N.$$

The first step is to estimate δ_h^k in terms of ρ_h^k and τ^k.

Lemma 5.2. *If $\lambda^*\Delta t<1/4$ and $A\in\mathcal{C}^0(0,T;\mathcal{V})\cap\mathcal{C}^1(0,T;L^2_r(\Omega_0))$, then*

$$\begin{aligned}(5.3)\quad &\max_{1\le k\le N}\|\delta_h^k\|^2_{L^2_r(\Omega_0)}\\ &\quad\le C\|\delta_h^0\|^2_{L^2_r(\Omega_0)}+C\Delta t\sum_{k=1}^N\left[\|\bar\partial\rho_h^k\|^2_{L^2_r(\Omega_0)}+\|\rho_h^k\|^2_{\widetilde H^1_r(\Omega_0)}+\|\tau^k\|^2_{L^2_r(\Omega_0)}\right],\end{aligned}$$

$$\begin{aligned}(5.4)\quad &\Delta t\sum_{k=1}^N\|\delta_h^k\|^2_{\widetilde H^1_r(\Omega)}\\ &\quad\le C\|\delta_h^0\|^2_{L^2_r(\Omega_0)}+C\Delta t\sum_{k=1}^N\left[\|\bar\partial\rho_h^k\|^2_{L^2_r(\Omega_0)}+\|\rho_h^k\|^2_{\widetilde H^1_r(\Omega_0)}+\|\tau^k\|^2_{L^2_r(\Omega_0)}\right],\end{aligned}$$

$$\begin{aligned}(5.5)\quad &\Delta t\sum_{k=1}^N\|\bar\partial\delta_h^k\|^2_{L^2_r(\Omega_0)}\\ &\quad\le C\|\delta_h^0\|^2_{\widetilde H^1_r(\Omega)}+C\Delta t\sum_{k=1}^N\left[\|\bar\partial\rho_h^k\|^2_{L^2_r(\Omega_0)}+\|\rho_h^k\|^2_{\widetilde H^1_r(\Omega_0)}+\|\tau^k\|^2_{L^2_r(\Omega_0)}\right].\end{aligned}$$

Proof. Because of the assumed regularity of A, testing Problems 5.1 and 3.1 with $Z_h\in\mathcal{V}_h\subset\mathcal{V}$ and subtracting allows us to write

$$\begin{aligned}(5.6)\quad &\left(\sigma\bar\partial\delta_h^k,Z_h\right)_{L^2_r(\Omega_0)}+a(t_k,\delta_h^k,Z_h)\\ &\qquad=-\left(\sigma\bar\partial\rho_h^k,Z_h\right)_{L^2_r(\Omega_0)}-c(t_k,\rho_h^k,Z_h)+\left(\sigma\tau^k,Z_h\right)_{L^2_r(\Omega_0)}\end{aligned}$$

for all $Z_h \in \mathcal{V}_h$ and $k = 1, \dots, N$.

On the other hand, the same argument leading to (5.1) in the proof of Theorem 5.1 leads to

$$\frac{1}{2\Delta t}\left[\|\sigma^{1/2}\delta_h^k\|^2_{L^2_r(\Omega_0)} - \|\sigma^{1/2}\delta_h^{k-1}\|^2_{L^2_r(\Omega_0)}\right] \le \left(\sigma\bar\partial\delta_h^k, \delta_h^k\right)_{L^2_r(\Omega_0)}.$$

By using the above inequality and Lemma 3.1, we obtain from (5.6) with $Z_h = \delta_h^k$ and a weighted Cauchy-Schwarz inequality,

$$\begin{aligned}\frac{1}{2\Delta t}\left[\|\sigma^{1/2}\delta_h^k\|^2_{L^2_r(\Omega_0)} - \|\sigma^{1/2}\delta_h^{k-1}\|^2_{L^2_r(\Omega_0)}\right] + \frac{\alpha}{2}\|\delta_h^k\|^2_{\widetilde{H}^1_r(\Omega)} - \lambda^*\|\sigma^{1/2}\delta_h^k\|^2_{L^2_r(\Omega_0)} \\ \le C\left[\|\bar\partial\rho_h^k\|^2_{L^2_r(\Omega_0)} + \|\rho_h^k\|^2_{\widetilde{H}^1_r(\Omega_0)} + \|\tau^k\|^2_{L^2_r(\Omega_0)}\right] + \frac{\alpha}{4}\|\delta_h^k\|^2_{L^2_r(\Omega_0)}.\end{aligned}$$

Summing from $k = 1$ to n $(1 \le n \le N)$ and a little algebra yields

$$\begin{aligned}&\|\sigma^{1/2}\delta_h^n\|^2_{L^2_r(\Omega_0)} - \|\sigma^{1/2}\delta_h^0\|^2_{L^2_r(\Omega_0)} + \frac{\alpha\Delta t}{2}\sum_{k=1}^n \|\delta_h^k\|^2_{\widetilde{H}^1_r(\Omega)} \\ &\le 2\lambda^*\Delta t\sum_{k=1}^n \|\sigma^{1/2}\delta_h^k\|^2_{L^2_r(\Omega_0)} + C\Delta t\sum_{k=1}^n\left[\|\bar\partial\rho_h^k\|^2_{L^2_r(\Omega_0)} + \|\rho_h^k\|^2_{\widetilde{H}^1_r(\Omega_0)} + \|\tau^k\|^2_{L^2_r(\Omega_0)}\right]\end{aligned}$$

and using that $\lambda^*\Delta t \le 1/4$,

$$\begin{aligned}\frac{1}{2}\|\sigma^{1/2}\delta_h^n\|^2_{L^2_r(\Omega_0)} + \frac{\alpha\Delta t}{2}\sum_{k=1}^n \|\delta_h^k\|^2_{\widetilde{H}^1_r(\Omega)} \\ \le \|\sigma^{1/2}\delta_h^0\|^2_{L^2_r(\Omega_0)} + 2\lambda^*\Delta t\sum_{k=1}^{n-1}\|\sigma^{1/2}\delta_h^k\|^2_{L^2_r(\Omega_0)} \\ + C\Delta t\sum_{k=1}^n\left[\|\bar\partial\rho_h^k\|^2_{L^2_r(\Omega_0)} + \|\rho_h^k\|^2_{\widetilde{H}^1_r(\Omega_0)} + \|\tau^k\|^2_{L^2_r(\Omega_0)}\right].\end{aligned}$$

Hence, by using the discrete Gronwall Lemma, we obtain for $n = 1, \dots, N$

$$\begin{aligned}&\|\sigma^{1/2}\delta_h^n\|^2_{L^2_r(\Omega_0)} \\ &\quad\le C\|\sigma^{1/2}\delta_h^0\|^2_{L^2_r(\Omega_0)} + C\Delta t\sum_{k=1}^n\left[\|\bar\partial\rho_h^k\|^2_{L^2_r(\Omega_0)} + \|\rho_h^k\|^2_{\widetilde{H}^1_r(\Omega_0)} + \|\tau^k\|^2_{L^2_r(\Omega_0)}\right],\end{aligned}$$

from which we conclude (5.3).

The second estimate follows by using the above inequality to estimate the terms $\|\sigma^{1/2}\delta_h^k\|^2_{L^2_r(\Omega_0)}$ in the right hand side of the previous one and straightforward computations.

For the third estimate, first we test (5.6) with $Z_h = \bar\partial\delta_h^k$ to obtain

$$\begin{aligned}&\left(\sigma\bar\partial\delta_h^k, \bar\partial\delta_h^k\right)_{L^2_r(\Omega_0)} + \widetilde{a}(\delta_h^k, \bar\partial\delta_h^k) \\ &\quad= -c(t_k, \delta_h^k, \bar\partial\delta_h^k) - \left(\sigma\bar\partial\rho_h^k, \bar\partial\delta_h^k\right)_{L^2_r(\Omega_0)} - c(t_k, \rho_h^k, \bar\partial\delta_h^k) + \left(\sigma\tau^k, \bar\partial\delta_h^k\right)_{L^2_r(\Omega_0)}.\end{aligned}$$

On the other hand, from the ellipticity of $\widetilde{a}$, it is immediate to show that

$$\widetilde{a}(\delta_h^k, \bar\partial\delta_h^k) \ge \frac{1}{2\Delta t}\left[\widetilde{a}(\delta_h^k, \delta_h^k) - \widetilde{a}(\delta_h^{k-1}, \delta_h^{k-1})\right].$$

By substituting this inequality in the previous identity and using a weighted Cauchy-Schwartz inequality, we arrive at

$$\begin{aligned}
&\Delta t\|\sigma^{1/2}\bar{\partial}\delta_h^k\|^2_{L^2_r(\Omega_0)} + \frac{1}{2}\left[\widetilde{a}(\delta_h^k,\delta_h^k) - \widetilde{a}(\delta_h^{k-1},\delta_h^{k-1})\right]\\
&\quad\le C\Delta t\left[\|\delta_h^k\|^2_{\widetilde{H}^1_r(\Omega_0)} + \|\bar{\partial}\rho_h^k\|^2_{L^2_r(\Omega_0)} + \|\rho_h^k\|^2_{\widetilde{H}^1_r(\Omega_0)} + \|\tau^k\|^2_{L^2_r(\Omega_0)}\right]\\
&\qquad + \frac{\Delta t}{2}\|\sigma^{1/2}\bar{\partial}\delta_h^k\|^2_{L^2_r(\Omega)}.
\end{aligned}$$

Now, we sum from $k=1$ to N to write

$$\begin{aligned}
&\Delta t\sum_{k=1}^{N}\|\sigma^{1/2}\bar{\partial}\delta_h^k\|^2_{L^2_r(\Omega_0)} + \widetilde{a}(\delta_h^N,\delta_h^N)\\
&\quad\le \widetilde{a}(\delta_h^0,\delta_h^0) + C\Delta t\sum_{k=1}^{N}\left[\|\delta_h^k\|^2_{\widetilde{H}^1_r(\Omega_0)} + \|\bar{\partial}\rho_h^k\|^2_{L^2_r(\Omega_0)} + \|\rho_h^k\|^2_{\widetilde{H}^1_r(\Omega_0)} + \|\tau^k\|^2_{L^2_r(\Omega_0)}\right].
\end{aligned}$$

Thus (5.5) follows from the ellipticity and the continuity of $\widetilde{a}$ and (5.4). □

Notice that in the previous lemma the estimate (5.5) differs from (5.3) and (5.4) in that it depends on $\|\delta_h^0\|_{\widetilde{H}^1_r(\Omega)}$, which in its turn depends on the chosen extension of A_h^0 to the whole Ω, namely, $A_h(0)$.

The following step is to obtain appropriate estimates for ρ_h^k and τ^k.

Lemma 5.3. *If $A\in H^1(0,T;H^2_r(\Omega)\cap\mathcal{V})$, then*

$$\Delta t\sum_{k=1}^{N}\|\bar{\partial}\rho_h^k\|^2_{L^2_r(\Omega_0)} + h^2\Delta t\sum_{k=0}^{N}\|\rho_h^k\|^2_{\widetilde{H}^1_r(\Omega)} \le Ch^4\|A\|^2_{H^1(0,T;H^2_r(\Omega))},$$

and if $A\in H^2(0,T;L^2_r(\Omega_0))$, then

$$\sum_{k=1}^{N}\|\tau^k\|^2_{L^2_r(\Omega_0)} \le C\Delta t\|A\|^2_{H^2(0,T;L^2_r(\Omega_0))}.$$

Proof. For the first estimate we use Barrow's rule, to write

$$\bar{\partial}\rho_h^k = \frac{1}{\Delta t}\int_{t^{k-1}}^{t^k}\partial_t\rho_h(t)\,dt.$$

Hence, using a Cauchy-Schwartz inequality and (4.5) we have

$$\Delta t\sum_{k=1}^{N}\|\bar{\partial}\rho_h^k\|^2_{L^2_r(\Omega_0)} \le \int_0^T\|\partial_t\rho_h(t)\|^2_{L^2_r(\Omega_0)}\,dt \le Ch^4\|A\|^2_{H^1(0,T;H^2_r(\Omega))}.$$

Moreover, since $\rho_h^k = A(t^k) - P_hA(t^k)$, from (4.3) we have

$$\Delta t\sum_{k=0}^{N}\|\rho_h^k\|^2_{\widetilde{H}^1_r(\Omega)} \le Ch^2\|A\|^2_{\mathcal{C}^0(0,T;H^2_r(\Omega))}.$$

Thus, we conclude the first estimate of the lemma from the last two inequalities.

For the second estimate we use a Taylor's formula in the definition of τ^k to write

$$\tau^k = \frac{1}{\Delta t}\int_{t^{k-1}}^{t^k}(t-t^{k-1})\partial_{tt}A(t)\,dt.$$

Hence, straightforward computations allow us to conclude the lemma. □

Now we are in a position to prove the main result of this paper. Analogously to what was done for the semi-discrete problem, we define the computed magnetic field (cf. (2.13) and (2.14))

$$\boldsymbol{B}_h^k := \mathbf{curl}(A_h^k \boldsymbol{e}_\theta)$$

and the computed current density in the workpiece (cf. (2.9) and (2.15))

$$\boldsymbol{J}_h^k := -\sigma\bar{\partial}A_h^k\boldsymbol{e}_\theta + \sigma\boldsymbol{v}\times\boldsymbol{B}_h^k \qquad \text{in } \Omega_0. \tag{5.7}$$

The following error estimates hold for this numerical method.

Theorem 5.4. *Let A be the solution to Problem 3.1 and assume it satisfies $A \in H^1(0,T;H_r^2(\Omega)\cap\mathcal{V})\cap H^2(0,T;L_r^2(\Omega_0))$. Let $\Delta t>0$ be such that $\lambda^*\Delta t<1/4$, with λ^* as in Lemma 3.1. Let A_h^k, $k=1,\dots,N$, be the solution to Problem 5.1, with initial data $A_h^0=\mathcal{I}_hA^0$. Let $\boldsymbol{B}$ be defined by (2.13) and (2.14) and $\boldsymbol{J}$ by (2.9) and (2.15). Let $\boldsymbol{B}_h^k$ and $\boldsymbol{J}_h^k$, $k=1,\dots,N$, be defined as above. Then, there exists a positive constant C independent of h, Δt, and A such that*

$$\max_{1\le k\le N}\|A(t^k)-A_h^k\|_{L_r^2(\Omega_0)} \le C\left[h\|A\|_{H^1(0,T;H_r^2(\Omega))}+\Delta t\|A\|_{H^2(0,T;L_r^2(\Omega_0))}\right],$$

$$\left[\Delta t\sum_{k=1}^N\|\boldsymbol{B}(t^k)-\boldsymbol{B}_h^k\|_{L_r^2(\Omega)}^2\right]^{1/2} \le C\left[h\|A\|_{H^1(0,T;H_r^2(\Omega))}+\Delta t\|A\|_{H^2(0,T;L_r^2(\Omega_0))}\right],$$

$$\left[\Delta t\sum_{k=1}^N\|\boldsymbol{J}(t^k)-\boldsymbol{J}_h^k\|_{L_r^2(\Omega_0)}^2\right]^{1/2} \le C\left[h\|A\|_{H^1(0,T;H_r^2(\Omega))}+\Delta t\|A\|_{H^2(0,T;L_r^2(\Omega_0))}\right].$$

Proof. By writing $A(t^k)-A_h^k=\delta_h^k+\rho_h^k$, from Lemmas 5.2 and 5.3, we obtain for all $k=1,\dots,N$

$$\|A(t^k)-A_h^k\|_{L_r^2(\Omega_0)} \le \|\delta_h^0\|_{L_r^2(\Omega_0)} + C\left[h\|A\|_{H^1(0,T;H_r^2(\Omega))}+\Delta t\|A\|_{H^1(0,T;H_r^2(\Omega))}\right].$$

On the other hand, the first term in the right hand side above is bounded as follows:

$$\|\delta_h^0\|_{L_r^2(\Omega_0)} \le \|A^0-A_h^0\|_{L_r^2(\Omega_0)}+\|\rho_h^0\|_{L_r^2(\Omega_0)} \le Ch\|A\|_{H^1(0,T;H_r^2(\Omega))}$$

where for the last inequality we have used that $A_h^0=\mathcal{I}_hA^0$, Theorem 4.1, and (4.3). Thus the first estimate of this theorem follows from the two inequalities above.

The proof of the second estimate is essentially identical.

The proof of the third one only differs in that $\|\delta_h^0\|_{\widetilde{H}_r^1(\Omega)}$ appears instead of $\|\delta_h^0\|_{L_r^2(\Omega_0)}$ when using Lemma 5.2. Then, from the definition of δ_h^0, we have

$$\|\delta_h^0\|_{\widetilde{H}_r^1(\Omega)} \le \|P_hA(0)-A(0)\|_{\widetilde{H}_r^1(\Omega)}+\|A(0)-A_h(0)\|_{\widetilde{H}_r^1(\Omega)} \le Ch\|A\|_{H^1(0,T;H_r^2(\Omega))},$$

where for the last inequality we have used (4.3) and Lemma 4.5. Using this inequality, the rest of the proof runs as those of the other estimates. □

6. Numerical experiments

The numerical method analyzed above has been implemented in a FORTRAN code. Notice that the terms including the velocity lead to a non-symmetric linear system at each time step. The corresponding systems have been solved by means of the SUPERLU algorithm [7]. In this section, we will report the results obtained by applying this code to different problems. First, we will present two tests which will allow us to check the order of convergence of the numerical method. Finally, we will apply the code to an electromagnetic problem arising from an industrial process: the metal sheet forming.

6.1. **Test with analytical solution.** First we consider a problem with known analytical solution, although it does not fit exactly in the theoretical framework considered in the previous sections, because the source current is supported in an extremely thin coil. This test will allow us to check the convergence results proved above. This example has been taken from [4] and [2] where it was used to analyze a similar problem in harmonic regime. In what follows we describe briefly the test; we refer the reader to [2, 4] for further details.

Let us consider an infinite cylinder consisting of a core metal surrounded by a crucible and an extremely thin coil. The multi-turn coil is modeled as a continuous single one with a uniform surface current density (see Figure 3). The current density is taken periodic in time. If we do not consider velocity terms, then the solution of the electromagnetic problem can be obtained in the whole space, even for an axisymmetric crucible composed by different materials, provided that the physical properties are constants in each material.

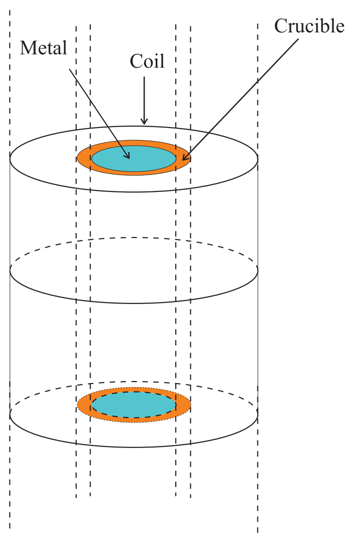

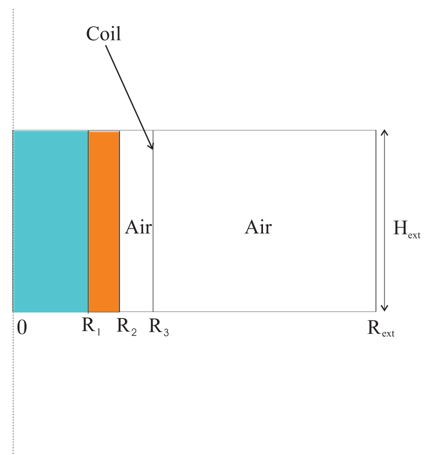

FIGURE 3. Analytical test. 3D and 2D sketches of the domain.

Since the current density is periodic in time, we assume that all the variables can be written as follows: $F(t,r,z) = \mathrm{Re}[e^{i\omega t}\widetilde{F}(r,z)]$, where $\omega > 0$ is the angular frequency of the source current. In such a case, for the problem described in Figure 3, the azimuthal component of the magnetic vector potential is given by $A(t,r,z) = \mathrm{Re}[e^{i\omega t}\widetilde{A}(r,z)]$, where

$$\widetilde{A}(r,z) = \begin{cases} \alpha_1 \,\mathrm{I}_1(r\sqrt{i\omega\mu\sigma}), & 0 < r < R_1, \\ \alpha_2 \,\mathrm{I}_1(r\sqrt{i\omega\mu\sigma}) + \beta_1 \,\mathrm{K}_1(r\sqrt{i\omega\mu\sigma}), & R_1 < r < R_2, \\ \alpha_3\mu_0 \dfrac{r}{2} + \dfrac{\beta_2}{r}, & R_2 < r < R_3, \\ \dfrac{\beta_{\mathrm{ext}}}{r}, & r > R_3, \end{cases}$$

with I_1 and K_1 being the first-order modified Bessel functions of the first and second kind, respectively. The coefficients μ and σ are taken constant in each material and the constants α_1, α_2, α_3, β_1, β_2, and β_{ext} are chosen so that $\widetilde{A}$ and $\frac{1}{\mu r}\frac{\partial(r\widetilde{A})}{\partial r}$ are continuous at $r = R_1$, $r = R_2$, and $r = R_3$.

We denote by R_{ext} and H_{ext} the width and height of the rectangular box enclosing the domain for the finite element computations (see Figure 3, again). For validation purposes, we have used exact Dirichlet boundary conditions, $\widetilde{A} = \beta_{\mathrm{ext}}/r$ at $r = R_{\mathrm{ext}}$, and homogeneous Neumann conditions on the horizontal edges (recall that, for $\widetilde{A} \in \widetilde{H}^1_r(\Omega)$, there also holds $\widetilde{A} = 0$ at $r = 0$).

The method has been used on several successively refined meshes by reducing the time step in a convenient way to analyze the convergence with respect to both, the mesh-size and the time step. With this aim, the numerical approximations have been compared with the analytical solution. As a first step, for each quantity A_h^k, $\boldsymbol{B}_h^k$, and $\boldsymbol{J}_h^k$, the dependence of the error on h and Δt was studied separately. To do this, first we fixed the time step to a sufficiently small value, so that the error practically depends only on the mesh-size. In this case we observed that the error of $\boldsymbol{B}_h^k$ reduces linearly with respect to h, while those of A_h^k and $\boldsymbol{J}_h^k$ reduces quadratically. Then, we fixed the mesh-size to a sufficiently small value for the time discretization error to prevail. In such a case we observed a linear dependence on Δt for all quantities.

We illustrate in Figures 4 and 5 the convergence behavior of the method for each of these quantities. These figures show log-log plots of the errors of A_h^k, $\boldsymbol{J}_h^k$, and $\boldsymbol{B}_h^k$ in the discrete norms considered in Theorem 5.4 versus the number of degrees of freedom (d.o.f.). To report in one only figure the simultaneous dependence on h and Δt, we proceeded in the following way: first, we chose initial values of h and Δt, so that the time and the space discretization errors were both of approximately the same size; secondly, for each of the successively refined meshes, we have taken values of Δt proportional either to h or to h^2, according to the previously observed dependence of the errors on the mesh-size.

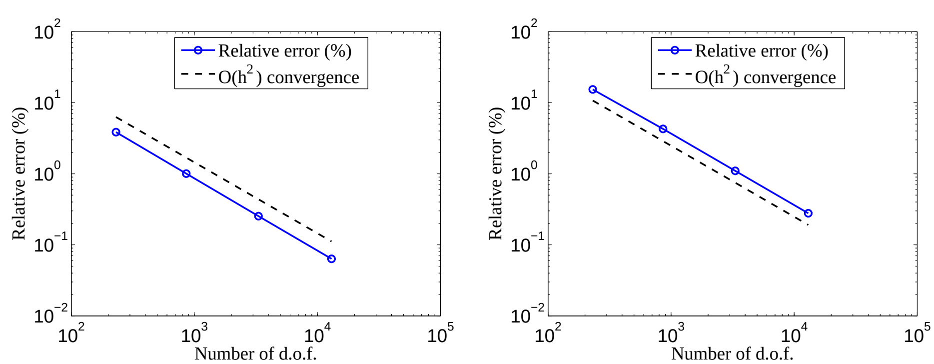

FIGURE 4. Analytical test. Relative errors for the magnetic vector potential $\max_{1\leq k\leq N} \|A(t^k) - A_h^k\|_{L^2_r(\Omega_0)}$ (left) and the current density $[\Delta t \sum_{k=1}^N \|\boldsymbol{J}(t^k) - \boldsymbol{J}_h^k\|^2_{L^2_r(\Omega_0)}]^{1/2}$ (right) versus number of d.o.f. (log-log scale), with $\Delta t = Ch^2$ in both cases

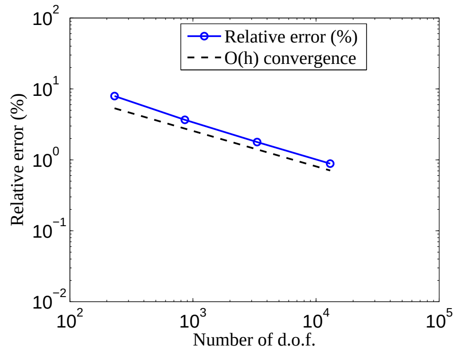

FIGURE 5. Analytical test. Relative errors for the magnetic induction $[\Delta t \sum_{k=1}^{N} \|\boldsymbol{B}(t^k) - \boldsymbol{B}_h^k\|^2_{L^2_r(\Omega)}]^{1/2}$ versus number of d.o.f. (log-log scale), with $\Delta t = Ch$.

A quadratic dependence on the mesh-size in the first two cases and a linear dependence in the third one can be clearly seen from these figures. Notice that the convergence behavior for all these quantities agrees with or improves the theoretically predicted order of convergence.

6.2. **Simulation of an induction heating furnace including a moving fluid.** The goal of this section is to analyze the convergence of the numerical method applied to a problem lying in the framework of the theoretical results and including the velocity term in the Ohm's law. We recall that in our analysis the domain of the conducting medium remains fixed throughout the process. This is what happens, for instance, in magnetohydrodynamic problems which involve a fluid in motion occupying a fixed domain [3]. In particular, we consider the simulation of a small induction furnace composed by a graphite crucible and containing silicon in motion inside. This example has been taken from [4] where it was solved in harmonic regimen. A sketch of the domain is presented in Figure 6, the geometrical data are described in more detail in [4]. In the present case, we assume that each turn of the coil has a periodic in time uniform current distribution with amplitude J_0, i.e., $J_{\mathrm{S}} := J_0 \cos(\omega t)$; these source data and the physical parameters are described in Table 1.

TABLE 1. Induction Furnace. Physical data.

Number of coil turns:	4
Amplitude of current density (in each turn) (J_0):	$3 \times 10^7\,\mathrm{A/m^2}$
Frequency (ω):	$50\,\mathrm{Hz}$
Electrical conductivity of silicon (σ):	$1234568\,(\mathrm{Ohm\,m})^{-1}$
Electrical conductivity of crucible (σ):	$240000\,(\mathrm{Ohm\,m})^{-1}$
Magnetic permeability of all materials (μ):	$4\pi 10^{-7}\,\mathrm{Hm}^{-1}$

The radial section of the domain containing melted silicon is a rectangle $[0, r_0] \times [z_0, z_1]$ with $r_0 = 0.021$, $z_0 = 0.004$, and $z_1 = 0.05$ all the lengths measured in meters. The velocity field in this domain has been taken as $\boldsymbol{v} = \mathbf{curl}(\varphi \boldsymbol{e}_\theta)$ with φ

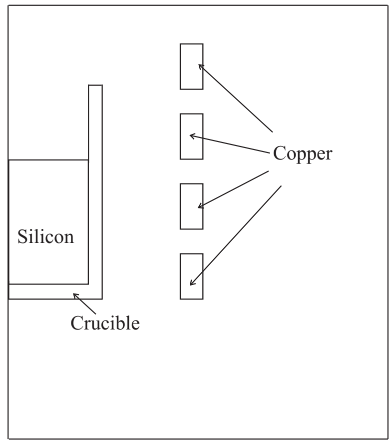

FIGURE 6. Induction Furnace. Sketch of the domain.

given by

$$\varphi = cr^2 (r - r_0)^2 (z - z_0)^2 (z - z_1)^2 .$$

The constant c has been taken large enough so that the electric current density due to this velocity be significant. In particular we have taken $c = 10^{14}$. Notice that $\boldsymbol{v}$ is divergence free and vanishes on the whole boundary of the rectangle.

The current arising from the velocity term is actually significant in this problem. In fact, this can be seen from Figure 7, where we plot the two components $\boldsymbol{J}^{\mathrm{E}} := \sigma\bar{\partial}A_h^k$ and $\boldsymbol{J}^{\mathrm{V}} := \sigma\boldsymbol{v} \times \boldsymbol{B}_h^k$ of the current density (cf. (5.7)).

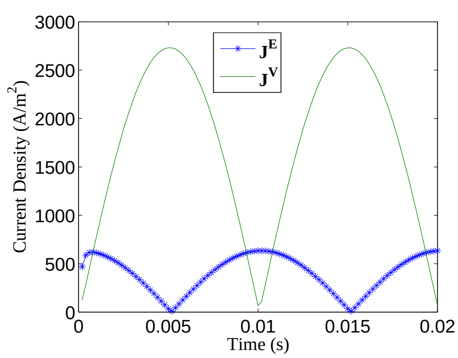

FIGURE 7. Induction Furnace. $\|\boldsymbol{J}^{\mathrm{E}}\|_{L^2_r(\Omega_0)}$ and $\|\boldsymbol{J}^{\mathrm{V}}\|_{L^2_r(\Omega_0)}$ versus time.

Since in this case there is no analytical solution to compare with, we have used as a reference solution the one obtained with the same finite element method for an extremely fine mesh. Numerical approximations $\boldsymbol{A}_h^k$, $\boldsymbol{B}_h^k$, and $\boldsymbol{J}_h^k$ obtained with several successively refined meshes have been compared with the reference one. In all cases we have used a time-step sufficiently small so that the errors arising from the time discretization be negligible with respect to the space discretization errors. Figure 8 and 9 show log-log plots of the corresponding relative errors.

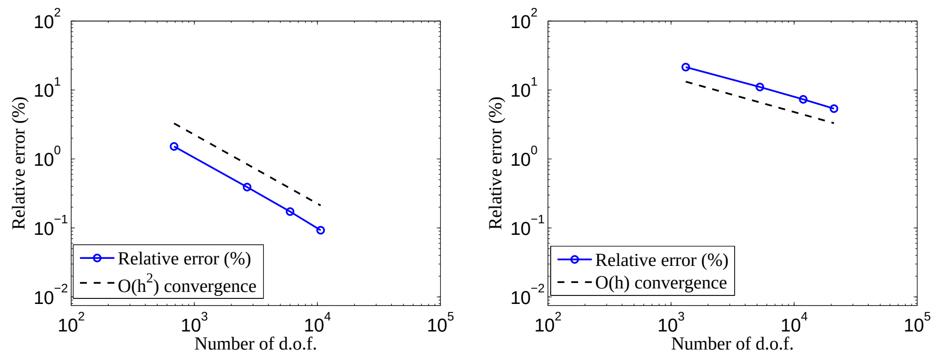

FIGURE 8. Induction furnace. Relative errors for the magnetic vector potential $\max_{1\le k\le N}\|A(t^k)-A_h^k\|_{L_r^2(\Omega_0)}$ (left) and the magnetic induction $[\Delta t\sum_{k=1}^N\|\boldsymbol{B}(t^k)-\boldsymbol{B}_h^k\|^2_{L_r^2(\Omega)}]^{1/2}$ (right) versus number of d.o.f. (log-log scale), with Δt sufficiently small.

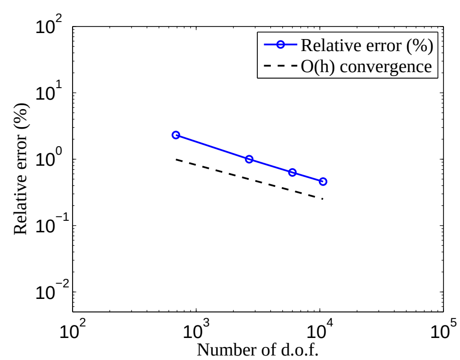

FIGURE 9. Induction furnace. Relative errors for the current density $[\Delta t\sum_{k=1}^N\|\boldsymbol{J}(t^k)-\boldsymbol{J}_h^k\|^2_{L_r^2(\Omega_0)}]^{1/2}$ versus number of d.o.f. (log-log scale), with Δt sufficiently small.

A linear order of convergence can be clearly observed for $\boldsymbol{B}_h^k$ and $\boldsymbol{J}_h^k$, as predicted by the theory. This is not the case for the magnetic potential A_h^k which converges quadratically, although only a linear order of convergence has been proved in Theorem 5.4. Even though this is just an auxiliary quantity, from the theoretical point of view it would be interesting to know whether such a quadratic convergence always holds.

6.3. **Simulation of an industrial application: An electromagnetic forming process.** Finally, we have used the numerical method to compute the current density and the Lorentz force in an example taken from an electromagnetic forming process. Electromagnetic forming (EMF) is a dynamic, high strain-rate forming method. In this process, deformation of the workpiece is driven by the interaction of a transient current induced in the same workpiece by a magnetic field generated by an adjacent coil ([8]).

In this section, we consider the geometry and physical data of the axisymmetric electromagnetic forming example described in [11] (see Figure 10 and Table 2), which corresponds to a classical benchmark problem (see [11, 16] for more details).

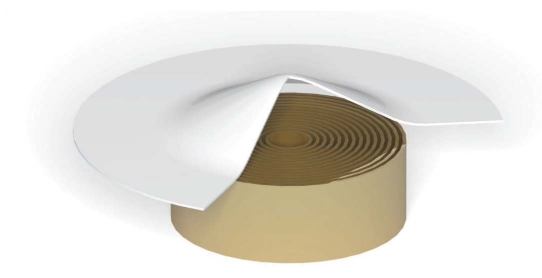

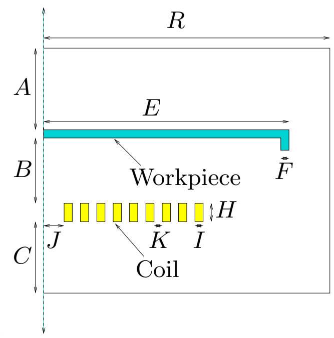

FIGURE 10. EMF. Geometry of the benchmark problem.

TABLE 2. EMF. Geometrical data and physical parameters:

Thickness of the workpiece (F):	0.0012 m
Height of the tool coil (H):	0.0115 m
Width of each turn coil (I):	0.0025 m
Distance between coil turns (K):	0.0003 m
Distance coil-workpiece (B):	0.002 m
Vertical distance from coil to bottom (C):	0.05 m
Vertical distance from workpiece to the top (A):	0.05 m
Width of the workpiece (E):	0.115 m
Width of the rectangular box (R):	0.2 m
Number of coil turns:	9
Electrical conductivity of metal (σ):	25900 $(\mathrm{Ohm\,m})^{-1}$
Magnetic permeability of all materials (μ):	$4\pi 10^{-7}\,\mathrm{Hm}^{-1}$

We are not able to compare in detail our results with those presented for the same benchmark problem in [16], because we have not included the deformation of the plate in the model. This deformation, which leads to an electromagnetic domain changing with time is the object of a forthcoming research. In the present case, we report some qualitative results obtained by using the geometrical data and the current source given in [11], which is shown in Figure 11. Notice that it corresponds to a source attaining very large values in a very short time: $10\,\mu$s.

We present in Figure 12 the axial component of the Lorentz force versus radius (left) and height (right) for a fixed time ($10\,\mu$s). The results are qualitatively very similar to those presented in Section 6 from [16].

ACKNOWLEDGMENT

The authors thank Rafael Muñoz-Sola for helpful discussions.

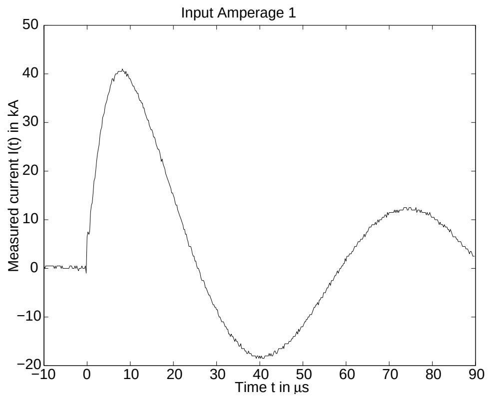

FIGURE 11. EMF. Current intensity (A) vs. time (μs).

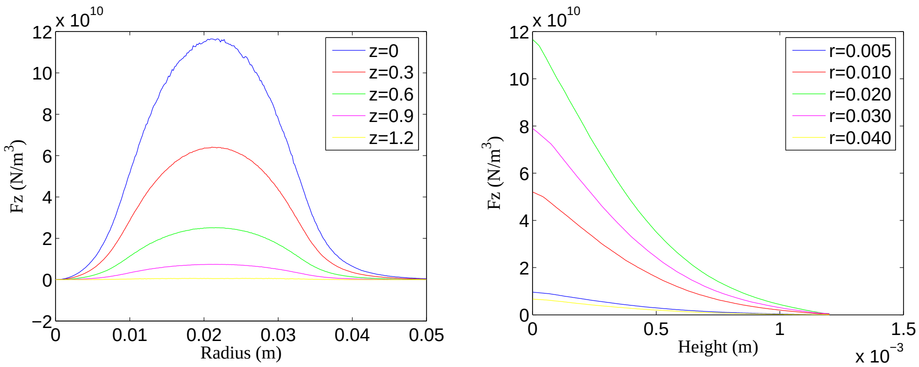

FIGURE 12. FEM. Axial component of the Lorentz force versus radius (left) and versus height (right) after 10 μs.

REFERENCES

1. F. Azzouz, B. Bendjima, M. Féliachi, and M. Latrèche, *Application of macro-element and finite element coupling for the behavior analysis of magnetoforming system*, IEEE Trans. Mag., **35** (1999) 1845–1848.
2. A. Bermúdez, D. Gómez, M.C. Muñiz, and P. Salgado, *Transient numerical simulation of a thermoelectrical problem in cylindrical induction heating furnaces*, Adv. Comput. Math., **26** (2007) 1–24.
3. A. Bermúdez, D. Gómez, M.C. Muñiz, P. Salgado, and R. Vázquez, *Numerical simulation of a thermo-electromagneto-hydrodynamic problem in an induction heating furnace*, Appl. Numer. Math., **59** (2009) 2082–2104.
4. A. Bermúdez, C. Reales, R. Rodríguez, and P. Salgado, *Numerical analysis of a finite element method to solve the axisymmetric eddy current model of an induction furnace*. IMA J. Numer. Anal. (doi: 10.1093/imanum/drn063; to appear).
5. C. Bernardi, M. Dauge, and Y. Maday, *Spectral Methods for Axisymmetric Problems*. Gauthier-Villars, Paris, 1999.
6. K.E. Brenan, S.L. Campbell, and L.R. Petzold, *Numerical Solution of Initial-Value Problems in Differential-Algebraic Equations*, SIAM, Philadelphia, 1996.
7. J.W. Demmel, S.C. Eisenstat, J.R. Gilbert, X. Li, and J. Liu, *A supernodal approach to sparse partial pivoting*, SIAM J. Matrix Anal. Appl., **20** (1999) 720–755.
8. A. El-Azab, M. Garnich, and A. Kapoor, *Modeling of the electromagnetic forming of sheet metals: state-of-art an future needs*, J. Mat. Process. Tech., **142** (2003) 744–754.

9. A. Ern and J. Guermond, *Theory and Practice of Finite Elements*, Springer-Verlag, New York, 2004.
10. J. Gopalakrishnan and J. Pasciak, *The convergence of V-cycle multigrid algorithms for axisymmetric Laplace and Maxwell equations*, Math. Comp., **75** (2006) 1697–1719.
11. M. Kleiner, A. Brosius, H. Blum, F. Suttmeier, M. Stiemer, B. Svendsen, J. Unger, and S. Reese, *Benchmark simulation for coupled electromagnetic-mechanical metal forming processes*, University of Dortmund, Chair of Forming Technology.
12. J.D. Lavers, *State of the art of numerical modeling for induction processes*, COMPEL, **27** (2008) 335–349.
13. B. Mercier and G. Raugel, *Resolution d'un problème aux limites dans un ouvert axisymétrique par éléments finis en r, z et séries de Fourier en θ*, RAIRO Anal. Numér., **16** (1982) 405–461.
14. A. Quarteroni and A. Valli, *Numerical Approximation of Partial Differential Equations*. Springer-Verlag, Berlin, 1994.
15. R.E. Showalter. *Monotone Operators in Banach Space and Nonlinear Partial Differential Equations*, American Mathematical Society, Providence, 1997.
16. M. Stiemer, O.J. Unger, B. Svendsen, and H. Blum, *Algorithmic formulation and numerical implementation of coupled electromagnetic-inelastic continuum models for electromagnetic metal forming*, Internat. J. Numer. Methods Engrg., **68** (2006) 1697–1719.
17. V. Thomée, *Galerkin Finite Element Methods for Parabolic Problems.* Springer-Verlag, Berlin, 2006.
18. A. Ženíšek, *Nonlinear Elliptic and Evolution Problems and Their Finite Element Approximations.* Academic Press, London, 1990.
19. M. Zlámal, *Finite element solution of quasistationary nonlinear magnetic field*, RAIRO Anal. Numér., **16** (1982) 161–191.
20. M. Zlámal, *Addendum to the paper "Finite element solution of quasistationary nonlinear magnetic field"*, RAIRO Anal. Numér., **17** (1983) 407–415.

Departamento de Matemática Aplicada, Universidade de Santiago de Compostela, 15706, Santiago de Compostela, Spain

E-mail address: `alfredo.bermudez@usc.es`

Departamento de Matemáticas y Estadísticas, Universidad de Córdoba, Colombia

Current address: Departamento de Ingeniería Matemática, Universidad de Concepción, Casilla 160-C, Concepción, Chile

E-mail address: `creales@ing-mat.udec.cl`

CI^{2}MA, Departamento de Ingeniería Matemática, Universidad de Concepción, Casilla 160-C, Concepción, Chile

E-mail address: `rodolfo@ing-mat.udec.cl`

Departamento de Matemática Aplicada, Universidade de Santiago de Compostela, 15706, Santiago de Compostela, Spain

E-mail address: `mpilar.salgado@usc.es`

Centro de Investigación en Ingeniería Matemática (CI^{2}MA)

PRE-PUBLICACIONES 2009 - 2010

2009-16 Gabriel N. Gatica, George C. Hsiao, Francisco J. Sayas: *Relaxing the hypotheses of the Bielak-MacCamy BEM-FEM coupling*

2009-17 Iuliu S. Pop, Florin A. Radu, Mauricio Sepúlveda, Octavio Vera: *Error estimates for the finite volume discretization for the porous medium equation*

2009-18 Raimund Bürger, Kenneth H. KARLSEN, Hector Torres, John D. Towers: *Second-order schemes for conservation laws with discontinuous flux modelling clarifier-thickener units*

2009-19 Maria G. Armentano, Claudio Padra, Rodolfo Rodríguez, Mario Scheble: *An hp finite element adaptive scheme to solve the Laplace model for fluid-solid vibrations*

2009-21 Carlos D. Acosta, Raimund Bürger, Carlos E. Mejia: *Monotone difference schemes stabilized by discrete mollification for strongly degenerate parabolic equations*

2009-22 Gabriel N. Gatica, Salim Meddahi: *Finite element analysis of a time harmonic Maxwell problem with an impedance boundary condition*

2009-23 Veronica Anaya, Mostafa Bendahmane, Mauricio Sepúlveda: *Mathematical and numerical analysis for predator-prey system in a polluted environment*

2009-24 Julio Aracena, Eric Fanchon, Marco Montalva, Mathilde Noual: *Combinatorics on update digraphs of discrete networks*

2010-01 Stefan Berres, Raimund Bürger, Rodrigo Garces: *Centrifugal settling of flocculated suspensions: A sensitivity analysis of parametric model functions*

2010-02 Mauricio Sepúlveda: *Stabilization of a second order scheme for a GKdV-4 equation modelling surface water waves*

2010-03 Lourenco Beirao-Da-Veiga, David Mora: *A mimetic discretization of the Reissner-Mindlin plate bending problem*

2010-04 Alfredo Bermúdez, Carlos Reales, Rodolfo Rodríguez, Pilar Salgado: *Mathematical and numerical analysis of a transient eddy current axisymmetric problem involving velocity terms*

Para obtener copias de las Pre-Publicaciones, escribir o llamar a: Director, Centro de Investigación en Ingeniería Matemática, Universidad de Concepción, Casilla 160-C, Concepción, Chile, Tel.: 41-2661324, o bien, visitar la página web del centro: http://www.ci2ma.udec.cl




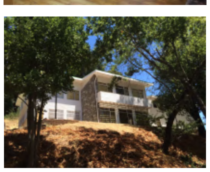
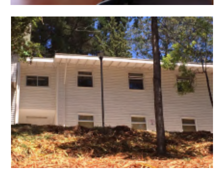

CENTRO DE INVESTIGACIÓN EN
INGENIERÍA MATEMÁTICA (CI^{2}MA)
Universidad de Concepción

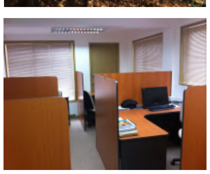
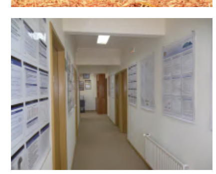

Casilla 160-C, Concepción, Chile
Tel.: 56-41-2661324/2661554/2661316
http://www.ci2ma.udec.cl